

An acute immune response underlies the benefit of cardiac stem cell therapy

<https://doi.org/10.1038/s41586-019-1802-2>

Received: 20 March 2018

Accepted: 8 November 2019

Published online: 27 November 2019

Ronald J. Vagnozzi¹, Marjorie Maillet¹, Michelle A. Sargent¹, Hadi Khalil¹, Anne Katrine Z. Johansen¹, Jennifer A. Schwaneckamp², Allen J. York¹, Vincent Huang¹, Matthias Nahrendorf³, Sakthivel Sadayappan² & Jeffery D. Molkentin^{1,4*}

Clinical trials using adult stem cells to regenerate damaged heart tissue continue to this day^{1,2}, despite ongoing questions of efficacy and a lack of mechanistic understanding of the underlying biological effect³. The rationale for these cell therapy trials is derived from animal studies that show a modest but reproducible improvement in cardiac function in models of cardiac ischaemic injury^{4,5}. Here we examine the mechanistic basis for cell therapy in mice after ischaemia–reperfusion injury, and find that—although heart function is enhanced—it is not associated with the production of new cardiomyocytes. Cell therapy improved heart function through an acute sterile immune response characterized by the temporal and regional induction of CCR2⁺ and CX3CR1⁺ macrophages. Intracardiac injection of two distinct types of adult stem cells, cells killed by freezing and thawing or a chemical inducer of the innate immune response all induced a similar regional accumulation of CCR2⁺ and CX3CR1⁺ macrophages, and provided functional rejuvenation to the heart after ischaemia–reperfusion injury. This selective macrophage response altered the activity of cardiac fibroblasts, reduced the extracellular matrix content in the border zone and enhanced the mechanical properties of the injured area. The functional benefit of cardiac cell therapy is thus due to an acute inflammatory-based wound-healing response that rejuvenates the infarcted area of the heart.

Initial animal studies with adult stem cells reported improved heart function through the formation of new cardiomyocytes by transdifferentiation of the injected cells^{6,7}. However, adult stem cell transdifferentiation was not observed in later studies^{4,5,8}, and clinical trials using adult stem cells in patients with acute myocardial infarction injury or decompensated heart failure have been indeterminate^{1,9}. The mechanistic basis for cell therapy therefore remains unclear, although a paracrine hypothesis has previously been proposed¹⁰. Here we focused on two types of primary adult stem cell: fractionated bone marrow mononuclear cells (MNCs)—which have extensively been used in human clinical trials²—and cardiac mesenchymal cells that express the receptor tyrosine kinase KIT, originally termed and referred to here as cardiac progenitor cells (CPCs)^{7,10}. We also examined the effect of injecting zymosan, a non-cellular and potent activator of the innate immune response¹¹. Isolated MNCs were a heterogeneous cell population that comprised all the major haematopoietic lineages—although monocytes and granulocytes were predominant (Extended Data Fig. 1a). CPCs expressed mesenchymal cell-surface markers but were negative for markers of haematopoietic or endothelial cells (Extended Data Fig. 1b).

Uninjured eight-week-old male and female C57Bl/6J mice received an intracardiac injection of strain-matched MNCs, zymosan or saline (Fig. 1a). Histological foci of acute inflammation were observed within

areas of cell or zymosan injection, as examined by confocal microscopy from heart sections three days, seven days or two weeks post-injection (Fig. 1b). Activated CD68⁺ macrophages were significantly increased within the area of injection after three and after seven days, with a diminishing effect by two weeks as the cells or zymosan were cleared (Fig. 1b, c). We did not observe any differences in neutrophil levels from dissociated hearts at three days after injection (Extended Data Fig. 1c).

To further profile the induction of macrophages owing to injection of MNCs or zymosan, we used *Ccr2-RFP*¹² and *Cx3cr1-GFP*¹³ knock-in mice to broadly distinguish the major subtypes of macrophage in the heart^{14,15}. We delivered unlabelled MNCs or zymosan into eight-week-old *Ccr2-RFP* × *Cx3cr1-GFP* mice by intracardiac injection (Fig. 1d). Uninjured (that is, noninjected) adult hearts showed GFP⁺ (CX3CR1⁺) macrophages throughout the myocardium, whereas RFP⁺ (CCR2⁺) macrophages were largely absent at baseline (Fig. 1e). After one day, areas of the heart injected with MNCs or zymosan showed a robust accumulation of CCR2⁺ macrophages, and CX3CR1⁺ macrophages began to expand in the periphery of the injected area (Fig. 1e). At three days, these CX3CR1⁺ macrophages had also expanded within the injection area along with the CCR2⁺ macrophages; this began to resolve by seven days after injection. Flow cytometry analysis from these mice at three days after injection also indicated a shift in the overall content of the macrophage subtypes from a largely CX3CR1⁺ CCR2⁻ population in the naive state to a mix of

¹Department of Pediatrics, University of Cincinnati, Cincinnati Children's Hospital Medical Center, Cincinnati, OH, USA. ²Department of Internal Medicine, Heart, Lung and Vascular Institute, University of Cincinnati, Cincinnati, OH, USA. ³Center for Systems Biology, Department of Imaging, Cardiovascular Research Center, Massachusetts General Hospital of the Harvard Medical School, Boston, MA, USA. ⁴Howard Hughes Medical Institute, Cincinnati Children's Hospital Medical Center, Cincinnati, OH, USA. *e-mail: jeff.molkentin@cchmc.org

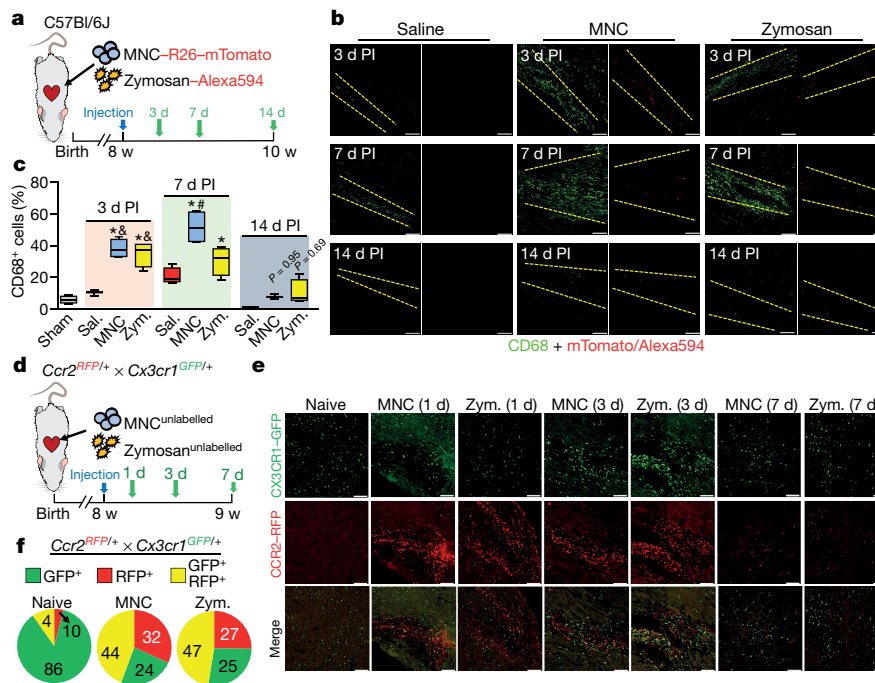


Fig. 1 | Cardiac cell injection causes local inflammation with the accumulation of distinct subtypes of macrophage. **a**, Experimental scheme using eight-week-old male and female C57Bl/6J mice subjected to intracardiac injection of strain-matched MNCs, Alexa Fluor 594-conjugated zymosan (zym.) or sterile saline (sal.). Sham-treated mice received thoracotomy, but no intracardiac injection. MNCs were isolated from *Rosa26-mTomato* mice on the C57Bl/6J background. **b**, Representative confocal immunohistochemistry micrographs of hearts showing activated CD68 macrophages (green), or the injected MNCs or zymosan (red). Dashed lines show injection sites. Images are from a minimum of 18 histological sections per mouse heart, assessed from $n = 3$ (saline at 3 days post-injection (PI), saline at 14 days post-injection and MNCs at 14 days post-injection) or $n = 4$ mice (all other groups). Scale bars, 100 μm . **c**, Quantification of CD68⁺ cells as a percentage of total cells (DAPI⁺), imaged at areas of injection from the groups described in **b**. Sample sizes for all groups are listed above in **b**. At 3 days, * $P < 0.0001$ versus sham, $^{\#}P = 0.0003$ (MNC versus saline), $^{\&}P = 0.0015$ (zymosan versus saline). At 7 days, * $P < 0.0001$ (MNC versus sham), * $P = 0.0005$ (zymosan versus sham), $^{\#}P < 0.0001$ (MNC versus saline). Significance was determined by one-way analysis of variance (ANOVA) with Tukey's post hoc test. Data are summarized as box-and-whisker

plots, indicating the median value (black bar inside box), 25th and 75th percentiles (bottom and top of box, respectively), and minimum and maximum values (bottom and top whisker, respectively). **d**, Experimental scheme using eight-week-old male and female *Ccr2-RFP* \times *Cx3cr1-GFP* knock-in mice to simultaneously visualize CCR2⁺ and CX3CR1⁺ subtypes of macrophage, after injection of MNCs or zymosan. **e**, Representative confocal micrographs from cardiac histological sections from MNC- or zymosan-injected mice, versus naive (non-injected) controls (minimum of 30 sections assessed per mouse heart from $n = 2$ naive control mice and $n = 3$ MNC- or zymosan-injected mice), showing endogenous RFP and GFP immunofluorescence from CCR2⁺ or CX3CR1⁺ cells, respectively, at the injection site over a seven-day time course. Scale bars, 100 μm . **f**, Distribution of CCR2⁺ and CX3CR1⁺ subtypes of macrophage in hearts at three days after injection. Pie charts reflect the proportion of RFP (CCR2⁺)- or GFP (CX3CR1⁺)-expressing cells, as well as CCR2⁺CX3CR1⁺ double-positive (yellow) cells detected by flow cytometry, as a percentage of total macrophages identified by staining for F4/80 and CD64. Data are from $n = 6$ MNC- and zymosan-injected mice or $n = 2$ naive (non-injected) mice.

enhanced numbers of CCR2⁺ and CCR2⁺CX3CR1⁺ (double-positive) macrophages with injection of MNCs or zymosan (Fig. 1f).

We also used immunohistochemistry to evaluate the ability of injected MNCs or zymosan to induce the formation of new cardiomyocytes (PCMI⁺) in the heart (Fig. 2a, b). We observed no appreciable increase in cardiomyocyte cell-cycle activity (Ki67⁺) versus saline-injected controls at the areas of injection, or distally across the entire tissue (Fig. 2c). Another proposed effect of cell therapy is the activation of endogenous CPCs; it has previously been determined that these can contribute to cardiac endothelial cell content after myocardial infarction injury¹⁶. We used a tamoxifen-inducible, *Kit^{MerCreMer}* \times *Rosa26-eGFP* lineage-tracing mouse strategy to examine endothelial cell formation from endogenous CPCs after injection of cells or zymosan (Figs. 2d, e). Notably, we did not observe transdifferentiation of injected MNCs or CPCs into cardiomyocytes or endothelial cells (Fig. 2f). However, two and six weeks after injection, eGFP⁺ endothelial cells were significantly increased at the injection sites in zymosan-treated hearts, but not in hearts injected with MNCs or CPCs (Fig. 2g, h). Zymosan persisted the longest within these hearts, whereas CPCs and MNCs were essentially cleared by two weeks after injection (Fig. 2e), which potentially explains

why zymosan was more effective. None of the treatments increased KIT⁺-derived endothelial cells in the distal areas of the heart.

We next injected strain-matched MNCs, CPCs, zymosan or saline on each side of the infarct border zone in C57Bl/6J mice one week after ischaemia-reperfusion (I-R) injury (Fig. 3a). Importantly, the injection of cells or zymosan into uninjured hearts did not alter left ventricular structure or function (Extended Data Fig. 2a-f). Injection of MNCs, CPCs or zymosan each significantly improved cardiac ventricular performance after I-R by two weeks after their injection, when compared with saline-injected controls (Fig. 3b). Of note, although the intracardiac injection procedure itself (saline) produced a mild inflammatory response (Extended Data Fig. 3a-e), it did not improve cardiac function after I-R (Extended Data Fig. 3f-i). Injection of cells or zymosan was also associated with improvements in left ventricular end-systolic volume, consistent with better cardiac function (Extended Data Fig. 4a). By contrast, there was no change in left ventricular end-diastolic volume (Extended Data Fig. 4b) or heart rate (Extended Data Fig. 4c) across any of the treatment groups at two weeks after therapy. Importantly, the observed functional benefit persisted for at least eight weeks after the injection of MNCs or zymosan (Fig. 3c).

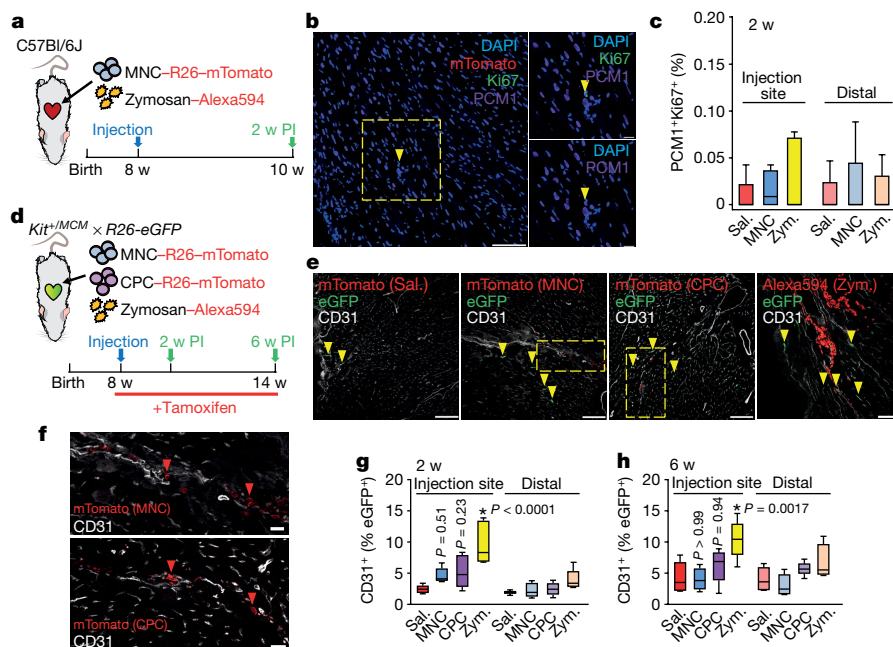


Fig. 2 | Cell or inflammatory therapy induces endothelial cell, but not cardiomyocyte, formation. **a**, Schematic of experiments performed in **b**, **c** in eight-week-old male and female C57Bl/6J mice that received intracardiac injection of MNCs, zymosan or saline, and were analysed two weeks later. **b**, Representative cardiac immunohistochemistry for Ki67 (green) and PCMI (purple) from MNC-injected hearts. DAPI (blue) shows nuclei. A minimum of 45 histological sections were analysed per mouse heart from $n = 4$ MNC-treated mice, or $n = 5$ mice for all other groups. The yellow box denotes an area shown at a higher magnification in the insets on the right. The yellow arrowhead denotes a cardiomyocyte with cell-cycle activity. Scale bars, 100 μm (left), 10 μm (right). **c**, Quantification of cardiomyocytes with cell-cycle activity (PCMI⁺Ki67⁺) as a percentage of all cardiomyocytes imaged (PCMI⁺) at two weeks after injection. Data are from a minimum of 45 cardiac histological sections analysed per mouse. $n = 4$ (MNC and at the injection site) or $n = 5$ mice for all other groups. **d**, Schematic of experiments performed in **e–h** using KIT lineage-tracing mice (*Kit^{MerCreMer/+} × Rosa26-eGFP*) injected with MNCs, CPCs, zymosan or saline, then analysed two or six weeks later. Tamoxifen was administered continuously (in chow), starting one day before cell injection. **e**, Representative confocal

immunohistochemistry images from hearts showing CD31⁺ endothelial cells (white) and injected MNCs, CPCs or zymosan (red). eGFP (green) shows *Kit*-allele-derived endothelial cells. Yellow arrowheads denote CD31⁺ endothelial cells that are also eGFP⁺. Scale bars, 100 μm . **f**, Larger insets of images shown in **e**, (within the boxed areas). Injected MNCs (top) or CPCs (bottom, rotated 90°) are shown with red arrowheads indicating mTomato⁺ cells that are negative for CD31 and lack known cardiomyocyte morphology. Scale bars, 20 μm . **g**, **h**, Quantification of the percentage of eGFP⁺ endothelial cells relative to total endothelial cells counted, either two weeks (**g**) or six weeks (**h**) post-injection. All data in **e–h** are from $n = 6$ (six weeks after zymosan injection) or $n = 5$ mice (all other groups). All *P* values in **g**, **h** were determined by one-way ANOVA with Tukey's post hoc test. All numerical data in this figure (**c**, **g**, **h**) are summarized as box-and-whisker plots, indicating the median value (black bar inside box), 25th and 75th percentiles (bottom and top of box, respectively), and minimum and maximum values (bottom and top whisker, respectively). Data and representative micrographs in **e–h** are from a minimum of 45 histological sections analysed per individual mouse heart from the numbers of mice indicated above.

We next treated mice with a high dosage of the broad-spectrum immunosuppressant cyclosporine A (CsA), which abrogated the restorative effects on cardiac function that were seen with injections of MNCs or zymosan after I–R injury (Fig. 3d). Administering clodronate liposomes acutely depleted macrophages and abolished the protective effect of the MNC injection after I–R in a similar manner to CsA treatment (Fig. 3e). Finally, injecting cellular debris from MNCs killed by freezing and thawing also improved cardiac function after I–R (Extended Data Fig. 4d).

Cardiac I–R injury itself is associated with a robust, temporal recruitment of discrete myeloid cell populations¹⁷, which we also observed using *Ccr2-RFP × Cx3cr1-GFP* mice (Fig. 3f). Of note, characterization of *Ccr2-RFP × Cx3cr1-GFP* mice at baseline using flow cytometry showed that over 90% of the CX3CR1⁺CCR2⁺ cells in the heart were tissue-resident CD169⁺ macrophages¹⁴, with a minor contribution of dendritic cells and neutrophils (Extended Data Fig. 5a–f). We also used *Ccr2*^{-/-} or *Cx3cr1*^{-/-} gene-targeted mice, and—although initial infarct sizes after I–R were not different among *Ccr2*^{-/-} or *Cx3cr1*^{-/-} mice and their strain-matched wild-type controls (not shown)—*Ccr2* deficiency partially improved cardiac function after I–R (Fig. 3h), consistent with previous reports^{18,19}. Moreover, cell therapy by MNC injection in mice that lack *Ccr2* imparted no further functional benefit beyond the improvement seen in these mice after I–R (Fig. 3h). The loss of *Ccr2* led to a reduction

in overall CD68⁺ cell content, specifically at the border zone of hearts after I–R—both with and without cell therapy (Fig. 3i). By comparison, *Cx3cr1*-null mice showed left ventricular dysfunction after I–R injury that was similar to wild-type controls, but these *Cx3cr1*-null mice no longer benefitted from MNC therapy and showed a much greater total inflammatory response (Fig. 3h, i). This result is consistent with a recent study that has shown that ablation of CX3CR1⁺ macrophages increases mortality and peri-infarct fibrosis after myocardial infarction in mice¹⁵. However, *Cx3cr1*-null mice show a GFP⁺ (expressed from the *Cx3cr1-GFP* allele) macrophage content after permanent occlusion myocardial infarction injury that is similar to that of control mice, as well as the same content of activated CD68⁺ macrophages in the infarct border zone at three days after myocardial infarction (Extended Data Fig. 6a–c). This observation is consistent with previous analyses of *Cx3cr1*-null mice, in which monocyte extravasation during peritonitis is unaffected¹³ and trafficking of tissue macrophages from the yolk sac during development is unaltered²⁰. Given these previous observations, the most likely explanation for our results is that CX3CR1 deficiency does not compromise tissue-resident macrophage content, but instead affects the function of these macrophages—resulting in greater tissue inflammation. Finally, the acute monocyte and neutrophil responses at three days after myocardial infarction were also not different between *Cx3cr1*-null mice and heterozygous *Cx3cr1-GFP* controls

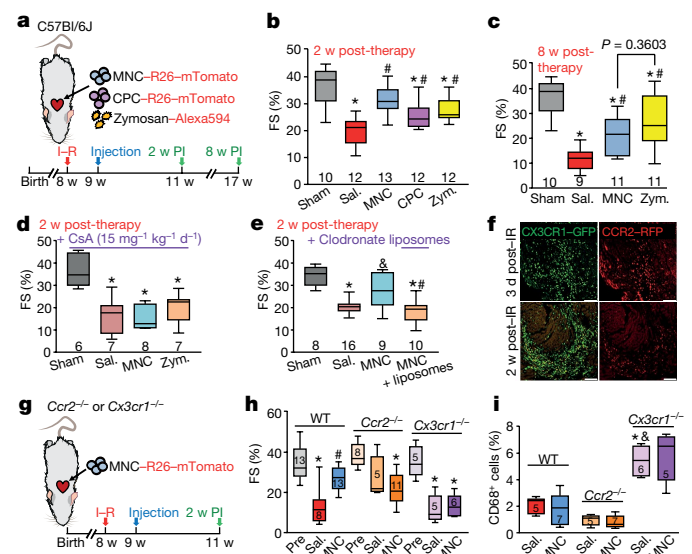


Fig. 3 | Cell or inflammatory therapy rejuvenates heart function after I-R. **a**, Schematic of experiments performed in **b**, **c**, in which eight-week-old male and female C57Bl/6J mice received 120 min of myocardial I-R injury, then (1 week later) intracardiac injection of MNCs, CPCs, zymosan or sterile saline flanking the injury area, followed by analysis two or eight weeks later. **b**, Fractional shortening (FS) as measured by echocardiography in the groups indicated, two weeks after cell or zymosan therapy. * $P < 0.0001$ (saline versus sham), * $P = 0.0002$ (CPC versus sham), * $P = 0.0019$ (zymosan versus sham), # $P < 0.0001$ (MNC versus saline), # $P = 0.0157$ (CPC versus saline), # $P = 0.0019$ (zymosan versus saline). **c**, Fractional shortening at eight weeks after cell or zymosan therapy. * $P < 0.0001$ (saline versus sham), * $P = 0.0002$ (MNC versus sham), * $P = 0.0086$ (zymosan versus sham), # $P = 0.0194$ (MNC versus saline), # $P = 0.0005$ (zymosan versus saline). Significance in **b**, **c** was determined by one-way ANOVA with Dunnett's post hoc test. The same sham group is shown in **b** and **c**, as these experiments were performed in parallel. **d**, Fractional shortening in post-I-R male and female mice that received CsA (15 milligrams per kilogram body weight per day) delivered by osmotic minipump, starting one day before MNC, zymosan or saline injection and continuing for two weeks after injection. * $P = 0.0004$ (saline versus sham), * $P = 0.0006$ (MNC versus sham), * $P = 0.0018$ (zymosan versus sham), all by one-way ANOVA with Dunnett's post hoc test. **e**, Fractional shortening in post-I-R male and female mice that received two injections of clodronate liposomes delivered intraperitoneally one day before MNC injection, and again five days after MNC injection. No difference between control and liposome treatment was observed in mice that received intracardiac injection of saline after I-R, so these groups were combined (denoted as saline). * $P < 0.0001$ (saline versus sham, or MNC + liposomes versus sham), # $P = 0.0276$ (MNC versus saline), # $P = 0.0042$ (MNC + liposomes versus MNC), all determined by one-way ANOVA with Dunnett's post hoc test. **f**, Confocal micrographs of histological sections at the infarct border zone of hearts from male and female *Ccr2-RFP* × *Cx3cr1-GFP* knock-in mice ($n = 2$ mice per group and time point, with a minimum of 10 sections assessed per mouse heart) at either three days or two weeks after I-R. Scale bars, 100 μm . **g**, Schematic of experiments performed in **h**, **i** in male and female *Ccr2*^{-/-} or *Cx3cr1*^{-/-} mice in the C57Bl/6J background that were subjected to I-R, and then injected with MNCs or sterile saline one week later. **h**, Fractional shortening in *Ccr2*^{-/-} or *Cx3cr1*^{-/-} mice or wild-type (WT) C57Bl/6J mice two weeks after cell injection, or non-injured mice (pre). * $P < 0.0001$ (wild type, saline versus pre), * $P = 0.0004$ (*Ccr2*^{-/-}, MNC versus pre), * $P = 0.0001$ (*Cx3cr1*^{-/-}, saline versus pre), * $P = 0.0002$ (*Cx3cr1*^{-/-}, MNC versus pre), # $P = 0.0030$ (wild type, MNC versus saline), all by one-way ANOVA with Tukey's post hoc test. **i**, Quantification of CD68⁺ cells as a percentage of total cells (DAPI) imaged at the infarct border zone, three weeks after I-R. * $P = 0.0001$ versus wild type and saline, # $P < 0.0001$ versus *Ccr2*^{-/-} and saline, all by one-way ANOVA with Tukey's post hoc test. The number of mice in each of the experimental groups is indicated below or within the respective graphs. All numerical data are summarized as box-and-whisker plots, indicating the median value (black bar inside box), 25th and 75th percentiles (bottom and top of box, respectively), and minimum and maximum values (bottom and top whisker, respectively).

(Extended Data Fig. 6d). However, we observed significantly greater mortality after myocardial infarction in *Cx3cr1*-null mice (Extended Data Fig. 6e), which suggests that CX3CR1⁺ cells have an important role in the later stages of infarct maturation (after day 3) and/or in the modulation of the fibrotic response, as has also recently been proposed¹⁵

Mechanistically, extracellular matrix content in the peri-infarct border zone was noticeably decreased with injection of MNCs around the I-R injury area (Fig. 4a, b). We also observed this decrease with the injection of non-viable MNCs, which suggests that it was primarily due to immunoreactivity—and not to active paracrine signalling (Fig. 4c). Notably, infarct strips from MNC-injected hearts produced a significantly greater change in passive force over increasing stretch, a profile that was more similar to that of the uninjured heart (change in initial length (L_0)) (Fig. 4d). This profile was also associated with a decrease in gene expression of several components of the extracellular matrix and genes that underlie the fibrotic response in MNC- versus saline-treated hearts after I-R injury (Fig. 4e). We repeated the force-lengthening assay on infarct strips from post-I-R hearts injected with zymosan, which showed an even larger improvement in passive force dynamics compared with the saline or MNC treatment (Extended Data Fig. 7a).

We next isolated bone marrow-derived macrophages or peritoneal macrophages from naive mice and cultured them on prefabricated collagen patches, followed by second harmonic generation microscopy to examine collagen organization (Fig. 4f). Bone marrow-derived macrophages and peritoneal macrophages each generated different patterns of collagen reorganization. To extend these observations, we used a collagen hybridizing peptide²¹ reagent, which detects immature or denatured collagen and areas of active remodelling, on injured mouse hearts (Extended Data Fig. 7b). Hearts from MNC- or zymosan-treated mice showed reactivity to the collagen hybridizing peptide that was coincident with regional localization of CCR2⁺ versus CX3CR1⁺ macrophages within the microenvironment of the infarct border zone (Extended Data Fig. 7c). Finally, we isolated CCR2⁺ or CX3CR1⁺ macrophages from hearts at seven days after I-R (Fig. 4g) and cultured them with freshly isolated cardiac fibroblasts for 72 h. Gene expression analysis revealed that CCR2⁺ macrophages increased fibroblast expression of smooth muscle α -actin (*Acta2*), lysyl oxidase (*Lox*) and collagen type I $\alpha 2$ (*Col1a2*) (Fig. 4h, i, k). By contrast, CX3CR1⁺ macrophages slightly reduced the expression of these genes but increased fibroblast expression of connective tissue growth factor (*Ctgf*, also known as *Ccn2*)²² (Fig. 4j). Together, these results demonstrate that specific subtypes of macrophage mobilized by cell therapy differentially affect the passive mechanical properties of the cardiac infarct area by influencing the activity of cardiac fibroblasts.

As suggested over a decade ago²³, we observed that the acute inflammatory response is a primary beneficial effect that underlies cell therapy in the injured heart after myocardial infarction. We identified a mechanism by which temporary stimulation of the intrinsic wound-healing cascade and select subtypes of macrophage positively affect the extracellular matrix around and within the infarcted region of the heart, such that functional performance is improved. These results are consistent with recent reports that demonstrate key functional distinctions between CCR2⁺ and CX3CR1⁺ CCR2⁻ macrophages in cardiac wound healing^{14,15}. In conclusion, our data suggest a need for the re-evaluation of current and planned clinical trials based on cardiac cell therapy to maximize the effects of the most prevalent underlying biological mechanism of action.

Online content

Any methods, additional references, Nature Research reporting summaries, source data, extended data, supplementary information, acknowledgements, peer review information; details of author contributions and competing interests; and statements of data and code availability are available at <https://doi.org/10.1038/s41586-019-1802-2>.

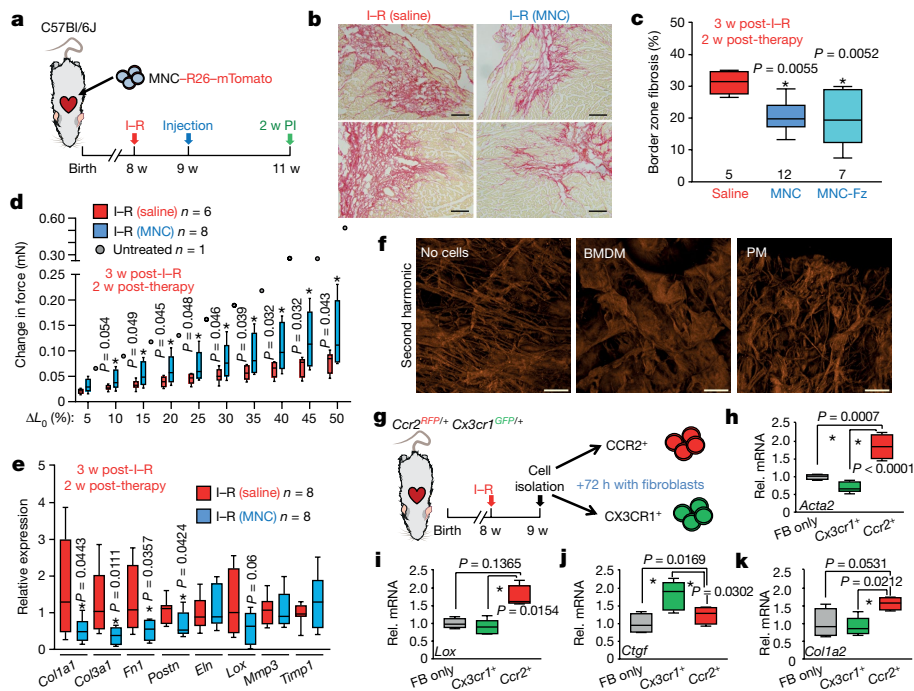


Fig. 4 | Cell therapy benefits the mechanical properties of the infarct via remodelling of the extracellular matrix. **a**, Schematic of experiments performed in **b–e**. **b**, Representative cardiac histological images stained with picosirius red from the infarct border zone of mice three weeks after I–R, subjected to MNC or saline injection. Fibrosis is shown in red. Scale bars, 100 μm . **c**, Quantification of fibrotic area at the infarct border zone in hearts treated with MNCs, MNCs killed by freezing and thawing (-Fz) or saline, three weeks after I–R. *P* values are shown in the panel and were calculated by one-way ANOVA with Tukey's post hoc test. Images in **b** and quantification in **c** are from $n = 5$ saline-treated mice, $n = 12$ MNC-treated mice or $n = 7$ mice treated with MNCs killed by freezing and thawing, with a minimum of 20 histological sections assessed from each individual mouse heart. **d**, Change in passive force generation over increasing stretch lengthening (per cent of L_0) in isolated infarct strips from MNC- or saline-treated hearts, three weeks after I–R. Exact *P* values are shown in the panel versus I–R and saline, and were calculated by Student's two-tailed *t*-test. Data from one untreated control heart (no I–R or cell therapy) are shown for comparison. **e**, mRNA expression levels by PCR with reverse transcription (RT–PCR) for selected genes associated with fibrosis and the extracellular matrix in isolated infarct regions from MNC or saline-treated hearts, three weeks after I–R. Exact *P* values are shown in the panel versus I–R and saline, by Student's two-tailed *t*-test. **f**, Representative confocal

micrographs of prefabricated collagen patches that were seeded and cultured for five days with either bone marrow-derived macrophages (BMDM) or peritoneal macrophages (PM) isolated from wild-type male and female mice, versus cell-free control patches cultured in medium. Fluorescence signal is from native type I and type II collagen using second harmonic generation microscopy. Scale bars, 100 μm . **g**, Schematic of experiments using activated cardiac macrophages isolated from post-I–R *Ccr2-RFP* \times *Cx3cr1-GFP* knock-in mice that were then cultured with isolated cardiac fibroblasts for 72 h. **h–k**, Fibroblast (FB) mRNA was used for RT–PCR to assess expression of *Acta2* (**h**), *Lox* (**i**), *Ctgf* (**j**) or *Col1a2* (**k**). Rel. mRNA, relative levels of mRNA. For **i**, **P* < 0.05 by Kruskal–Wallis with Dunn's multiple comparisons test. For all other panels, **P* < 0.05 by one-way ANOVA with Tukey's post hoc test (exact *P* values are shown in the panels). All numerical data are summarized as box-and-whisker plots, indicating the median value (black bar inside box), 25th and 75th percentiles (bottom and top of box, respectively), and minimum and maximum values (bottom and top whisker, respectively). Micrographs in **f** are representative of five collagen patches seeded with cells pooled from $n = 4$ mice (2 male and 2 female). Data in **g–k** are from 4–5 replicates generated from fibroblasts isolated from $n = 10$ wild-type mice (6 male and 4 female) and macrophages isolated from $n = 6$ *Ccr2-RFP* \times *Cx3cr1-GFP* heterozygous knock-in mice (3 male and 3 female).

- Nguyen, P. K., Rhee, J. W. & Wu, J. C. Adult stem cell therapy and heart failure, 2000 to 2016: a systematic review. *JAMA Cardiol.* **1**, 831–841 (2016).
- Fernández-Avilés, F. et al. Global position paper on cardiovascular regenerative medicine. *Eur. Heart J.* **38**, 2532–2546 (2017).
- Epstein, J. A. A time to press reset and regenerate cardiac stem cell biology. *JAMA Cardiol.* **4**, 95–96 (2019).
- Zwetsloot, P. P. et al. Cardiac stem cell treatment in myocardial infarction: a systematic review and meta-analysis of preclinical studies. *Circ. Res.* **118**, 1223–1232 (2016).
- Tompkins, B. A. et al. Preclinical studies of stem cell therapy for heart disease. *Circ. Res.* **122**, 1006–1020 (2018).
- Orlic, D. et al. Bone marrow cells regenerate infarcted myocardium. *Nature* **401**, 701–705 (2001).
- Beltrami, A. P. et al. Adult cardiac stem cells are multipotent and support myocardial regeneration. *Cell* **114**, 763–776 (2003).
- Eschenhagen, T. et al. Cardiomyocyte regeneration: a consensus statement. *Circulation* **136**, 680–686 (2017).
- A futile cycle in cell therapy. *Nat. Biotechnol.* **35**, 291 (2017).
- Sanganalmath, S. K. & Bolli, R. Cell therapy for heart failure: a comprehensive overview of experimental and clinical studies, current challenges, and future directions. *Circ. Res.* **113**, 810–834 (2013).
- Pillemer, L., Blum, L., Pensky, J. & Lepow, I. H. The requirement for magnesium ions in the inactivation of the third component of human complement (C3) by insoluble residues of yeast cells (zymosan). *J. Immunol.* **71**, 331–338 (1953).
- Saederup, N. et al. Selective chemokine receptor usage by central nervous system myeloid cells in *CCR2*-red fluorescent protein knock-in mice. *PLoS ONE* **5**, e13693 (2010).
- Jung, S. et al. Analysis of fractalkine receptor CX₃CR1 function by targeted deletion and green fluorescent protein reporter gene insertion. *Mol. Cell. Biol.* **20**, 4106–4114 (2000).
- Bajpai, G. et al. Tissue resident CCR2⁻ and CCR2⁺ cardiac macrophages differentially orchestrate monocyte recruitment and fate specification following myocardial injury. *Circ. Res.* **124**, 263–278 (2019).
- Dick, S. A. et al. Self-renewing resident cardiac macrophages limit adverse remodeling following myocardial infarction. *Nat. Immunol.* **20**, 29–39 (2019).
- van Berlo, J. H. et al. c-kit⁺ cells minimally contribute cardiomyocytes to the heart. *Nature* **509**, 337–341 (2014).
- Nahrendorf, M. et al. The healing myocardium sequentially mobilizes two monocyte subsets with divergent and complementary functions. *J. Exp. Med.* **204**, 3037–3047 (2007).
- Kaikita, K. et al. Targeted deletion of CC chemokine receptor 2 attenuates left ventricular remodeling after experimental myocardial infarction. *Am. J. Pathol.* **165**, 439–447 (2004).
- Leuschner, F. et al. Therapeutic siRNA silencing in inflammatory monocytes in mice. *Nat. Biotechnol.* **29**, 1005–1010 (2011).
- Stremmel, C. et al. Yolk sac macrophage progenitors traffic to the embryo during defined stages of development. *Nat. Commun.* **9**, 75 (2018).
- Hwang, J. et al. In situ imaging of tissue remodeling with collagen hybridizing peptides. *ACS Nano* **11**, 9825–9835 (2017).
- Brigstock, D. R. Regulation of angiogenesis and endothelial cell function by connective tissue growth factor (CTGF) and cysteine-rich 61 (CYR61). *Angiogenesis* **5**, 153–165 (2002).
- Thum, T., Bauersachs, J., Poole-Wilson, P. A., Volk, H. D. & Anker, S. D. The dying stem cell hypothesis: immune modulation as a novel mechanism for progenitor cell therapy in cardiac muscle. *J. Am. Coll. Cardiol.* **46**, 1799–1802 (2005).

Publisher's note Springer Nature remains neutral with regard to jurisdictional claims in published maps and institutional affiliations.

© The Author(s), under exclusive licence to Springer Nature Limited 2019

Methods

Mice

This study was performed entirely in mice, using transgenic models that are commercially available as described later in this section. No human subjects or human material were used. All experiments involving mice were approved by the Institutional Animal Care and Use Committee (IACUC) at Cincinnati Children's Hospital under protocol IACUC2018-0047. All procedures were performed in compliance with institutional and governmental regulations under PHS Animal Welfare Assurance number D16-00068 (A3108-01). The generation and characterization of mice carrying the tamoxifen-inducible MerCreMer recombinase cDNA within the *Kit* allele (*Kit^{MerCreMer/+}*), and reporter mice carrying the Cre-regulated loxP-stop cassette and eGFP within the *Rosa26* gene locus, *Rosa26-eGFP* (R-GFP), have previously been described¹⁶. All the other mouse strains were purchased from The Jackson Laboratory, as follows: C57Bl/6J; (no. 000664), constitutive mTomato-expressing mice targeted in the *Rosa26* locus for MNC or CPC isolation; (*B6.129(Cg)-Gt(ROSA)26Sortm4(CTB-tdTomato,-EGFP)Luo/J*, no. 007676), *Ccr2*-gene-deleted mice; (*B6.129S4-Ccr2tm1lfc/J*, no. 004999), *Cx3cr1-GFP* knock-in mice (*Cx3cr1* homozygotes are nulls); (*B6.129P-Cx3cr1tm1litt/J*, no. 005582) and *Ccr2*RFP knock-in mice; (*B6.129(Cg)-Ccr2tm2.1lfc/J*, no. 017586). Both male and female mice were used in all experiments, at age ranges indicated in the figures and text for each experiment. Mice were housed with mice of the same sex at a maximum of 4 mice per cage in a specific-pathogen-free, temperature-controlled vivarium under a 12-h light–dark cycle with ad libitum access to food and water. Randomization was not performed, because mice are genetically identical, housed together and of the same age ranges and sex ratios.

Preparation of cell or inflammatory therapies

To generate MNCs for injection, whole bone marrow was first isolated by flushing dissected femurs and tibiae of 10–12-week-old *Rosa26-mTomato*-expressing mice or C57Bl/6J mice with 10 ml of sterile Hanks Balanced Salt Solution (HBSS, Fisher Scientific no. SH3058801) + 2% bovine growth serum (BGS, Fisher Scientific, no. SH3054103) + 2 mM EDTA, as previously described²⁴. This suspension was then filtered through a 40- μ m mesh strainer (Fisher Scientific no. 22-363-547), centrifuged at 400g for 10 min at 4 °C, resuspended in 3 ml of sterile saline and layered on top of 4 ml of Ficoll Paque Plus (GE Healthcare no. 17-1440-02). Cells were then centrifuged at 2,500g for 30 min at 4 °C in a swinging bucket rotor centrifuge without brakes. MNCs were isolated by removal of the resulting thin mononuclear cell layer (the second layer from the top). Total MNCs were counted with a haemocytometer, washed twice with sterile saline and resuspended in sterile saline at a final concentration of either 2.5×10^6 cells per millilitre (for injection into uninjured hearts, a final dose 50,000 cells) or 7.5×10^6 cells per millilitre (for injection into post-I–R hearts, a final dose 150,000 cells). A higher dose of cells (MNCs or CPCs, see 'Mouse procedures') was used in post-I–R hearts to account for greater cell loss in the setting of damaged myocardium and to align with previous studies^{4,5}. The full intracardiac injection procedure is described in 'Mouse procedures'. Cell viability was tested by incubating an aliquot of the MNC suspension with eFluor 450 Fixable Viability Dye (eBioscience no. 65-0863-18) and was found to be over 90% viable at the time of injection. All MNC preparations for injection were combined from an equal number of male and female mice. For experiments that used non-viable MNCs (frozen and thawed), this final MNC suspension was split into two equal aliquots. One aliquot was placed immediately at –80 °C for 10 min, followed immediately by incubation at 55 °C for 10 min, and this was repeated for a total of 3 freeze–thaw cycles.

To generate CPCs for injection, hearts from 10–12-week-old *Rosa26-mTomato*-expressing male and female mice were rapidly excised and briefly rinsed in cold 1 \times PBS. Single-cell suspensions from these hearts were prepared according to previously published protocols^{25,26} with

minor modifications. The atria were removed, and the ventricles were minced on ice using surgical scissors into approximately 2-mm pieces (8–10 pieces per mouse heart). Each dissociated ventricle was transferred into 2 ml of digestion buffer in 1 well of a 12-well tissue culture plate. Digestion buffer consisted of 2 mg/ml collagenase type IV (Worthington, no. LS004188), 1.2 U/ml dispase II (Roche, no. 10165859001) and 0.9 mM CaCl₂, in 1 \times HBSS. Tissues were incubated at 37 °C for 20 min with gentle rotation followed by manual trituration 12–15 times with a 10-ml serological pipette, such that all the tissue pieces were able to pass through the pipette. The tissues were settled by sedimentation and the supernatant was passed through a 40- μ m mesh strainer and stored on ice. Two millilitres of fresh digestion buffer was added, followed by 2 additional rounds of incubation, trituration and replacement of supernatant with fresh digestion buffer, except trituration was performed with a 5-ml serological pipette for round 2 and a 1-ml p1000 pipette tip (USA Scientific, no. 1112-1720) for round 3. The pooled supernatant from the 3 rounds of digestion was washed with sterile PBS and centrifuged at 200g for 20 min at 4 °C in a swinging bucket rotor centrifuge without brakes. The pellet was resuspended in flow cytometry sorting buffer, consisting of 1 \times HBSS supplemented with 2% BGS and 2 mM EDTA, and incubated with anti-KIT microbeads (Miltenyi Biotec no. 130-091-224) for 20 min at 4 °C with gentle rotation. The suspensions were washed twice with sorting buffer and KIT⁺ cells were enriched via positive selection over Miltenyi Biotec LS columns (no. 130-042-401) using benchtop magnetic cell separation (MACS) according to the manufacturer's instructions. Cells isolated via positive MACS selection for KIT were cultured in DMEM–F12–Glutamax medium (Gibco no. 10565-018) supplemented with 10% fetal bovine serum (Sigma, no. F2442), 0.2% insulin–transferrin–selenium (Lonza, no. 17-838Z), 20 ng/ml basic recombinant human fibroblast growth factor (Promega, no. G5071), 10³ U/ml leukaemia inhibitor factor (Millipore, no. ESG1106), 20 ng/ml epidermal growth factor (Sigma, no. E9644) and 1% penicillin–streptomycin (Fisher Scientific, no. 30-002-CI).

KIT⁺ isolated cells from the heart are referred to as CPCs (as previously named), although recent data would suggest that these cells transdifferentiate only into endothelial cells, and not cardiomyocytes, in vivo^{3,8,16}. KIT⁺ isolated cells were expanded in culture for 12–15 passages before being used for injection, at which point cells were washed 3 times with sterile saline, trypsinized, counted and resuspended in sterile saline at a final concentration of either 2.5×10^6 cells per millilitre (for injection into uninjured hearts, a final dose 50,000 cells) or 7.5×10^6 cells per millilitre (for injection into post-I–R hearts, a final dose 150,000 cells). As with MNCs, suspensions comprised pooled CPCs from an equal number of male and female mice.

Alexa Fluor 594-conjugated zymosan, or unconjugated zymosan, were purchased from Thermo Fisher (zymosan A (*Saccharomyces cerevisiae*) BioParticles, Alexa Fluor 594 conjugate, no. Z-23374, zymosan A (*S. cerevisiae*) BioParticles, unlabelled, no. Z2849). A suspension of either 1 mg/ml (for injection into uninjured hearts, a final dose of 10 μ g) or 2 mg/ml (for injection into post-I–R hearts, a final dose of 20 μ g) was prepared for injection in sterile saline according to the manufacturer's instructions. Zymosan dosing was extrapolated from a previous study using injection into neonatal mouse hearts²⁷. A higher dose of zymosan was used in post-I–R hearts to enable comparisons with MNC- and CPC-treated animals.

Mouse procedures

To deliver cell or inflammatory therapies by intracardiac injection, mice were anaesthetized using isoflurane inhalation (to effect) and intubated, and a left lateral thoracotomy was performed. A 25- μ l gas-tight syringe (Hamilton, no. 7654-01) fitted with a 33-gauge needle (Hamilton, no. 7803-05) was used for injections. For experiments in mice without injury, 20 μ l of MNCs at a concentration of 2.5×10^6 cells per millilitre (50,000 cells in total) was injected over 3 regions of the left ventricle (6.7 μ l per injection). For experiments with zymosan,

10 μ l of a 1 mg/ml suspension was injected over 3 regions of the left ventricle (3.3 μ l per injection, 10 μ g zymosan in total). Injections were equidistant along the anterior wall of the left ventricle, with the needle entering just parallel to the long axis of the ventricle to avoid entering the left ventricular chamber. For experiments with injections occurring after cardiac injury, two injections were performed, one on either side of the infarct zone. Twenty microlitres total of MNCs or CPCs at a concentration of 7.5×10^6 cells per millilitre (150,000 cells total) was injected (10 μ l per injection). For experiments with zymosan, 10 μ l total of a 2 mg/ml suspension was injected (5 μ l per injection, 20 μ g zymosan in total). A greater number of cells and higher amount of zymosan were injected into the injured heart compared with the uninjured (naive) heart, because of less retention and a greater turnover of the cells or zymosan owing to the infarction injury. The sham procedure for intracardiac injection consisted of anaesthesia, intubation and thoracotomy as performed for the previously described myocardial infarction procedure²⁸. The chest was then immediately closed, and mice recovered.

To induce cardiac injury, we used a modified surgical model of I–R via temporary left coronary artery ligation as previously described²⁸, in which 120 min of ischaemia was used before inducing reperfusion, which gave more complete killing of the ischaemic zone and greater reproducibility. After each surgical procedure (I–R or intracardiac injection), animals were given post-operative analgesics (buprenorphine, 0.1 milligram per kilogram body weight) and allowed to recover until the experimental time points indicated, at which point mice were then further analysed, or tissue was collected. For experiments with permanent-occlusion myocardial infarction, the same procedure was performed except the ligature was not released. Randomization was not performed because the mice used here are genetically identical, housed together and of the same age ranges and sex ratios. A discussion of blinding and sample elimination considerations can be found in ‘Statistical information and experimental rigour (blinding)’.

Infarct size and area-at-risk after I–R was determined using triphenyl tetrazolium chloride and Evans blue staining, as previously described²⁸. In experiments using immunosuppression via CsA, mice were anaesthetized with 2% isoflurane inhalation to effect, and osmotic minipumps (Alzet, no. 1002) were implanted subcutaneously on the left lateral side of the mouse. Minipumps were loaded with CsA (Neoral, Novartis, NDC 0078-0274-22) dissolved in Cremophor EL (Sigma, no. C5135) such that 15 milligrams CsA per kilogram of body weight was delivered per day²⁹. In experiments using acute macrophage ablation, mice were administered 2 doses of 0.2 ml each of clodronate liposomes (Clophosome, no. F70101C-N) via intraperitoneal injection, one day before cell therapy and again on day 5 after cell therapy. Liposomes were kept on ice until administration and were rapidly mixed by inversion to deliver a uniform suspension. Control mice were injected with 0.2 ml of sterile saline. In experiments using *Kit^{MerCreMer/+} × Rosa26-eGFP* genetic lineage-tracing mice, tamoxifen was administered as previously described¹⁶ via ad libitum feeding with premanufactured tamoxifen chow (tamoxifen citrate 40 milligrams per kilogram body weight per day, Envigo, no. TD.1308603) for the time indicated in each individual experiment. For echocardiographic analysis of cardiac structure and function, mice were anaesthetized with 2% isoflurane inhalation to effect and analysed using a Vevo2100 instrument (VisualSonics) with an 18–38-MHz transducer as previously described³⁰. Randomization was not performed because mice are genetically identical and of the same age ranges. A discussion of blinding and sample elimination considerations can be found in ‘Mice’ and ‘Statistical information and experimental rigour (blinding)’.

Histology and immunohistochemistry

Primary antibodies and dilutions used for immunohistochemistry are listed in Supplementary Table 1. For histological analysis, mice were

anaesthetized by isoflurane inhalation and killed by cervical dislocation. The chest was opened, and the heart was flushed with cold cardioplegia solution (1 M KCl in 1 \times PBS) via cardiac apical insertion of a 25-gauge needle. The left atrium was cut to allow drainage of blood from the heart, and mice were briefly perfused with cold fixative (4% paraformaldehyde in sodium phosphate buffer, pH 7.4) through the apex of the heart. Tissues were excised, flushed with fixative and incubated in cold fixative for 3.5 h at 4 °C with gentle rotation. Tissues were washed 3 times in cold 1 \times PBS and then cryopreserved by incubation in 30% sucrose in 1 \times PBS overnight at 4 °C with gentle rotation. Tissues were then embedded in TissueTek optimal cutting temperature medium (VWR, no. 25608-930) and flash-frozen at –80 °C. Five-micrometre cryosections were cut using a Leica CM1860 cryostat.

Picrosirius red staining was performed with a kit from Abcam (ab150681), as per the manufacturer’s instructions. High-magnification images of hearts stained with picrosirius red were captured at 200 \times magnification using an Olympus BX51 microscope equipped with a single chip colour CCD camera (DP70) and DP controller software (Olympus America, v.3.1.1.). Border zone fibrosis was quantified as the percentage of picrosirius red-stained area over total tissue area analysed, as previously described³¹.

All detection of genetic reporter-driven mTomato, RFP, GFP or eGFP expression was performed using endogenous fluorescence without antibody labelling. Immunohistochemistry was performed on cardiac cryosections as previously described^{16,26} with the following modifications (see Supplementary Table 1 for primary antibodies and dilutions). Alexa Fluor fluorochrome-conjugated secondary antibodies were used at a 1:200 dilution for visualization (Life Technologies). For immunohistochemistry using antibodies against PCMI, antigen retrieval was first performed by incubation with 1% SDS for 5 min at room temperature with gentle rotation. PCMI antibody was used to specifically identify cardiomyocytes in heart tissue sections. Histological cardiac sections were washed thoroughly in 1 \times PBS before proceeding. For immunohistochemistry using the collagen hybridizing peptide (CHP) (3Helix, no. BIO300), a stock solution of 15 μ M biotin-conjugated CHP was prepared according to the manufacturer’s instructions. The solution was heated to 80 °C for 5 min to denature the peptide, as previously described²¹, followed by rapid cooling on ice and incubation on tissue sections overnight at 4 °C. Sections were then washed and processed for secondary antibody staining with fluorophore-conjugated streptavidin antibody used at a 1:200 dilution for visualization (Life Technologies). Confocal microscopy and image acquisition were performed using a Nikon Eclipse Ti inverted microscope equipped with a Nikon A1R confocal running NIS Elements AR 4.50.

Passive force measurements

Tissue strips from the infarct region of the left ventricle (or the left ventricular free wall for uninjured hearts) were dissected using a Zeiss Discovery V8 dissection microscope. Tissues were cut into 3 mm (length) \times 2-mm (width) strips, and 3 or 4 strips were cut from each infarct region of the left ventricle. These strips contained scar and a small region of border zone on each end. Tissue strips were maintained in M199 media (Corning Cellgro, 10-060-CV) with no supplementation throughout the procedure of force measurements. Tissue strips were attached to aluminium t-clips (Kem-Mil, no. 1870) and mounted onto a permeabilized muscle fibre test apparatus (Aurora Scientific, Model: 802D-160-322) initially set to zero tension. Cardiac tissue length was then increased 5% over 50 ms, held for 450 ms and then stretched again from 5% to 50% in intervals of 5% with no period of relaxation, and force was monitored using DMC v600A software (Aurora Scientific). Change in force was calculated as the difference between maximum force generated after the 50-ms pull and the minimum force achieved after each time period. Minimum force was calculated when the rate of force decay was zero by solving for the derivative of the best-fit trend line, which was a second-degree polynomial equation.

RT-PCR from isolated infarct tissues

Tissue strips isolated from the infarct region as described in 'Passive force measurements' were homogenized with a Precellys 24 homogenizer (Bertin Instruments no. 03119.200.RD000) and RNA was isolated by using the RNeasy fibrous tissue kit according to the manufacturer's instructions (Qiagen no. 74704). One microgram of total RNA was reverse-transcribed using random oligo-dT primers and a Verso cDNA synthesis kit (Thermo Fisher Scientific no. AB1453A) according to the manufacturer's instructions. Real-time PCR was performed using Sso Advanced SYBR Green (BioRad no. 1725274) according to the following programme: one cycle of 95 °C for 10 min, one cycle of 95 °C for 15 s, 40 cycles of 95 °C for 15 s, 57 °C for 10 s and 62 °C for 30 s, and one cycle of 62 °C for 30 s. *Gapdh* expression was used for normalization. Primer sequences used are included in Supplementary Table 2.

Flow cytometry and cell sorting

For analysis of surface markers on MNCs or CPCs, cells were resuspended in 1× HBSS supplemented with 2% BGS and 2 mM EDTA and incubated with fluorophore- or biotin-conjugated primary antibodies (Supplementary Table 1) for 20 min at 4 °C with gentle rotation. Cells were then washed twice with 1× HBSS + 2% BGS and 2 mM EDTA. For detection of biotinylated antibodies, cells were incubated with streptavidin-conjugated BV421 (BD Horizon no. 563259) for 15 min at 4 °C with gentle rotation and then washed twice with 1× HBSS + 2% BGS and 2 mM EDTA. Samples were analysed using a BD FACSCanto running BD FACSDiVa V.8.0 software (BD Biosciences) and using the following laser configuration: blue (488 nm), yellow-green (561 nm) and red (635 nm). Analysis and quantification were performed using FlowJo v.10 (Tree Star).

For flow cytometry analysis of whole heart cardiac immune cell content, single-cell suspensions were first prepared using enzymatic dissociation and trituration as described in 'Preparation of cell or inflammatory therapies'. Mice were anaesthetized by 2% isoflurane inhalation to effect and killed by cervical dislocation. Hearts were rapidly excised and briefly rinsed in cold cardioplegic solution (1M KCl in 1× PBS) before enzymatic dissociation. The pellet resulting from dissociation was resuspended in 1 ml of red blood cell lysis buffer (150 mM NH₄Cl, 10 mM KHCO₃ and 0.1 mM Na₂EDTA) and incubated at room temperature for 5 min. Samples were then centrifuged at 400g for 10 min at 4 °C and resuspended in 1× HBSS supplemented with 2% BGS and 2 mM EDTA. Cells were incubated with fluorophore-conjugated primary antibodies for 20 min at 4 °C with gentle rotation, washed twice with 1× HBSS and analysed using a BD LSRFortessa running BD FACSDiVa v.8.0 software (BD Biosciences) and using the following laser configuration: UV (355 nm), violet (405 nm), blue (488 nm), yellow-green (561 nm) and red (635 nm) to detect fluorophore-conjugated antibodies and/or endogenous RFP and GFP signal from *Ccr2-RFP* × *Cx3cr1-GFP* mice. Analysis and quantification were performed using FlowJo v.10 (Tree Star).

For isolation of cardiac CCR2⁺ or CX3CR1⁺ macrophages by fluorescence-activated cell sorting, hearts from *Ccr2-RFP* × *Cx3cr1-GFP* mice at 7 days after I-R injury were isolated and dissociated to single-cell suspensions as described in 'Preparation of cell or inflammatory therapies' for isolation of CPCs, except that the digestion solution was made in DMEM + 2% BGS and 1% penicillin-streptomycin instead of HBSS. Isolated cells were sorted by fluorescence-activated cell sorting using a Sony SH800S benchtop cell sorter in a BSL-2 biosafety cabinet. Endogenous RFP and GFP fluorescence were detected using 4 collinear lasers and CCR2⁺ (RFP⁺GFP⁻) or CX3CR1⁺ (GFP⁺RFP⁻ or RFP⁺) cells were sorted into 1.5-ml Eppendorf tubes containing DMEM + 10% BGS and 1% penicillin-streptomycin. Cells were then cultured on isolated cardiac fibroblasts as described in 'Cardiac fibroblast and macrophage co-culture'.

Cardiac fibroblast isolation

Hearts were excised from ten eight-week-old male and female C57Bl/6 mice, and the ventricles and septum were isolated, rinsed in ice-cold PBS and minced into small pieces using sterile microscissors. Tissue fragments were digested in DMEM + 2% BGS and 1% penicillin-streptomycin containing type 2 collagenase (100 units per millilitre; LS004177, Worthington) for 20 min at 37 °C under gentle agitation. The digested tissue was triturated repeatedly to promote tissue dissociation. Dense fragments settled for 2 min and the supernatant, containing the cardiac fibroblasts, was collected and spun at 100g for 5 min. The cell pellet was resuspended in 10 ml of DMEM + 10% BGS and 1% penicillin-streptomycin and kept on ice. This process was repeated three times, until all the tissue was adequately digested. To remove cardiomyocytes and cell debris, cell suspensions were spun at 30g, followed by centrifugation of the supernatant at 100g. The final cell pellet containing the cardiac fibroblasts was resuspended in DMEM + 10% BGS and 1% penicillin-streptomycin and pre-incubated on 0.1% gelatin-coated plates for 2 h to allow fibroblast adherence before replenishment of the cell culture medium.

Cardiac fibroblast and macrophage co-culture

Isolated cardiac fibroblasts were split into 24-well 0.1% gelatin-coated plates at a seeding density of 15,000 cells per well and allowed to adhere overnight. Macrophage subtypes (CCR2⁺ and CX3CR1⁺ cells) isolated as described in 'Flow cytometry and cell sorting' were then seeded onto these cardiac fibroblasts at a density of 10,000 macrophages per 15,000 fibroblasts. Control fibroblasts received an equivalent amount of culture medium containing no macrophages. Adherence was verified the following day by fluorescence microscopy for RFP or GFP. Cells were isolated 72 h later for mRNA quantification.

mRNA isolation and qRT-PCR from cultured cardiac fibroblasts

Total RNA was purified from cultured cells with TRIzol reagent (Fisher Scientific no. 15596018) according to the manufacturer's instructions. Two hundred nanograms of RNA was reverse-transcribed to cDNA using the Verso cDNA synthesis kit (Thermo Fisher Scientific no. 277.97). Quantitative PCR was performed using SsoAdvanced Universal SYBR Green Supermix (BioRad no. 1725274) and assayed in duplicate, according to the manufacturer's instructions in a CFX96 PCR system. Primer sequences are included in Supplementary Table 2. All data were normalized to *Gapdh* (verified to not deviate between samples).

Macrophage culture on fibrillar collagen patches

Pre-sterilized resorbable collagen membranes (Ace Surgical Supply no. 509-3040) were cut into circles of a uniform thickness and a diameter of 6 mm, and then placed into 96-well plates. Bone marrow or peritoneal macrophages were isolated as previously described^{32,33} and cultured in DMEM + 10% BGS and 1% penicillin-streptomycin. Cells were then seeded onto the collagen patches at a density of 10,000 cells per patch. Control patches were incubated in culture medium without macrophages. Five biological replicates were performed per group. After five days in culture, fibrillar collagen assembly was analysed by second harmonic generation microscopy using a Nikon A1R multiphoton upright confocal microscope equipped with a tuneable Coherent Chameleon II TiSapphire IR laser set to 840 nm. Three images were randomly taken per patch and assessed by a blinded investigator to select the representative images for each group.

Statistical information and experimental rigour (blinding)

All statistical tests used and graphical depictions of data (means and error bars, or box and whisker plots) are defined within the figure legends for the respective data panels. Exact *n* values for all experiments with statistical analysis are included in the figure legends or within the figure itself. For comparisons between two groups, unpaired or

Student's two-tailed *t*-tests were performed as noted within figure legends. For comparisons between more than two groups, a one-way ANOVA with Tukey's or Dunnett's post hoc test was performed as noted within figure legends. $P < 0.05$ was considered as statistically significant. Data in Fig. 4i used a Kruskal–Wallis test with Dunn's multiple comparisons test, as these data did not follow a normal distribution. All other data were found to follow a normal distribution as determined by the Shapiro–Wilk normality test or Kolmogorov–Smirnov test ($\alpha = 0.05$). For experiments involving I–R surgery, the number of mice that received surgery was determined based on previous experimentation in the laboratory, which demonstrated a peri-operative surgical mortality rate of 20%. Only mice that did not survive a given surgical procedure, or which were found at the time of I–R surgery to have incomplete reperfusion (failure of slipknot suture release), were excluded from analysis; otherwise no exclusions occurred. Randomization of mice within a group to receive a given surgical procedure (I–R versus sham) or treatment (saline versus cells or zymosan) was not needed because the mice were genetically identical and were littermates, although equal sex ratios and age ranges were maintained. Echocardiographic analysis, quantification of eGFP⁺ endothelial cells, quantification of cardiomyocytes in cell cycle, measures of fibrosis, measures of tissue passive force, in vivo and in vitro gene expression analysis, and analysis of collagen organization in culture were conducted by investigators blinded to experimental treatment or procedure. Quantification of macrophage content by immunohistochemistry was performed using automated fluorescence threshold analysis in NIS Elements 4.50.

Reporting summary

Further information on research design is available in the Nature Research Reporting Summary linked to this paper.

Data availability

All raw data generated or analysed in this study are available from the corresponding author upon reasonable request. Original source data used to generate graphs in each of the figures and Extended Data figures are available as Microsoft Excel data sheet files from the corresponding author.

24. Schwanekamp, J. A., Lorts, A., Vagnozzi, R. J., Vanhoutte, D. & Molkentin, J. D. Deletion of periostin protects against atherosclerosis in mice by altering inflammation and extracellular matrix remodeling. *Arterioscler. Thromb. Vasc. Biol.* **36**, 60–68 (2016).
25. Pinto, A. R. et al. Revisiting cardiac cellular composition. *Circ. Res.* **118**, 400–409 (2016).
26. Vagnozzi, R. J. et al. Genetic lineage tracing of Sca-1⁺ cells reveals endothelial but not myogenic contribution to the murine heart. *Circulation* **138**, 2931–2939 (2018).
27. Han, C. et al. Acute inflammation stimulates a regenerative response in the neonatal mouse heart. *Cell Res.* **25**, 1137–1151 (2015).
28. Kaiser, R. A. et al. Targeted inhibition of p38 mitogen-activated protein kinase antagonizes cardiac injury and cell death following ischemia-reperfusion in vivo. *J. Biol. Chem.* **279**, 15524–15530 (2004).
29. Sussman, M. A. et al. Prevention of cardiac hypertrophy in mice by calcineurin inhibition. *Science* **281**, 1690–1693 (1998).
30. Liu, R. et al. Cardiac-specific deletion of protein phosphatase 1 β promotes increased myofilament protein phosphorylation and contractile alterations. *J. Mol. Cell. Cardiol.* **87**, 204–213 (2015).
31. Khalil, H. et al. Fibroblast-specific TGF- β -Smad2/3 signaling underlies cardiac fibrosis. *J. Clin. Invest.* **127**, 3770–3783 (2017).
32. Zhang, X., Goncalves, R. & Mosser, D. M. The isolation and characterization of murine macrophages. *Curr. Protoc. Immunol.* **14**, 14.11–14.114 (2008).
33. Davies, L. C., Jenkins, S. J., Allen, J. E. & Taylor, P. R. Tissue-resident macrophages. *Nat. Immunol.* **14**, 986–995 (2013).

Acknowledgements This work was supported by grants from the National Institutes of Health to J.D.M., S.S. and M.N. J.D.M. was supported by the Howard Hughes Medical Institute and the American Heart Association (19MERIT34370048). R.J.V. was supported by a National Research Service Award from the NIH (F32 HL128083) and a Career Development Award from the American Heart Association (19CDA34670044). All flow cytometric data were acquired using equipment maintained by the Research Flow Cytometry Core in the Division of Rheumatology at Cincinnati Children's Hospital Medical Center.

Author contributions J.D.M. and R.J.V. conceived the study. R.J.V., M.M., M.A.S., H.K., A.K.J., J.A.S., A.J.Y. and V.H. performed experiments and generated all the data shown in the manuscript. S.S. provided oversight and technical help along with J.A.S. in measuring myocardial scar mechanical properties. M.N. provided theoretical assessment of the project and advice in experimental design. J.D.M. and R.J.V. interpreted the data and wrote the manuscript.

Competing interests The authors declare no competing interests.

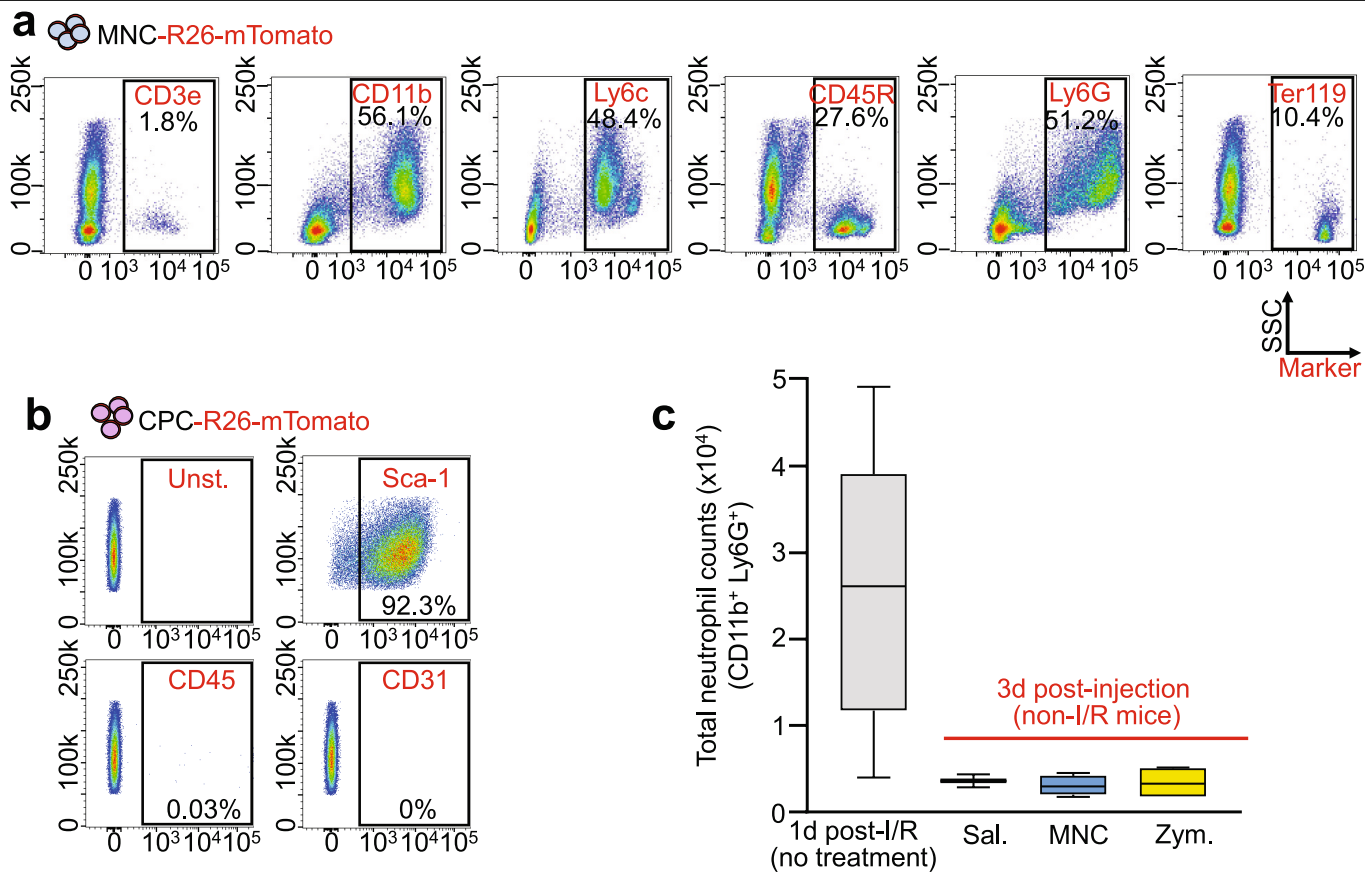
Additional information

Supplementary information is available for this paper at <https://doi.org/10.1038/s41586-019-1802-2>.

Correspondence and requests for materials should be addressed to J.D.M.

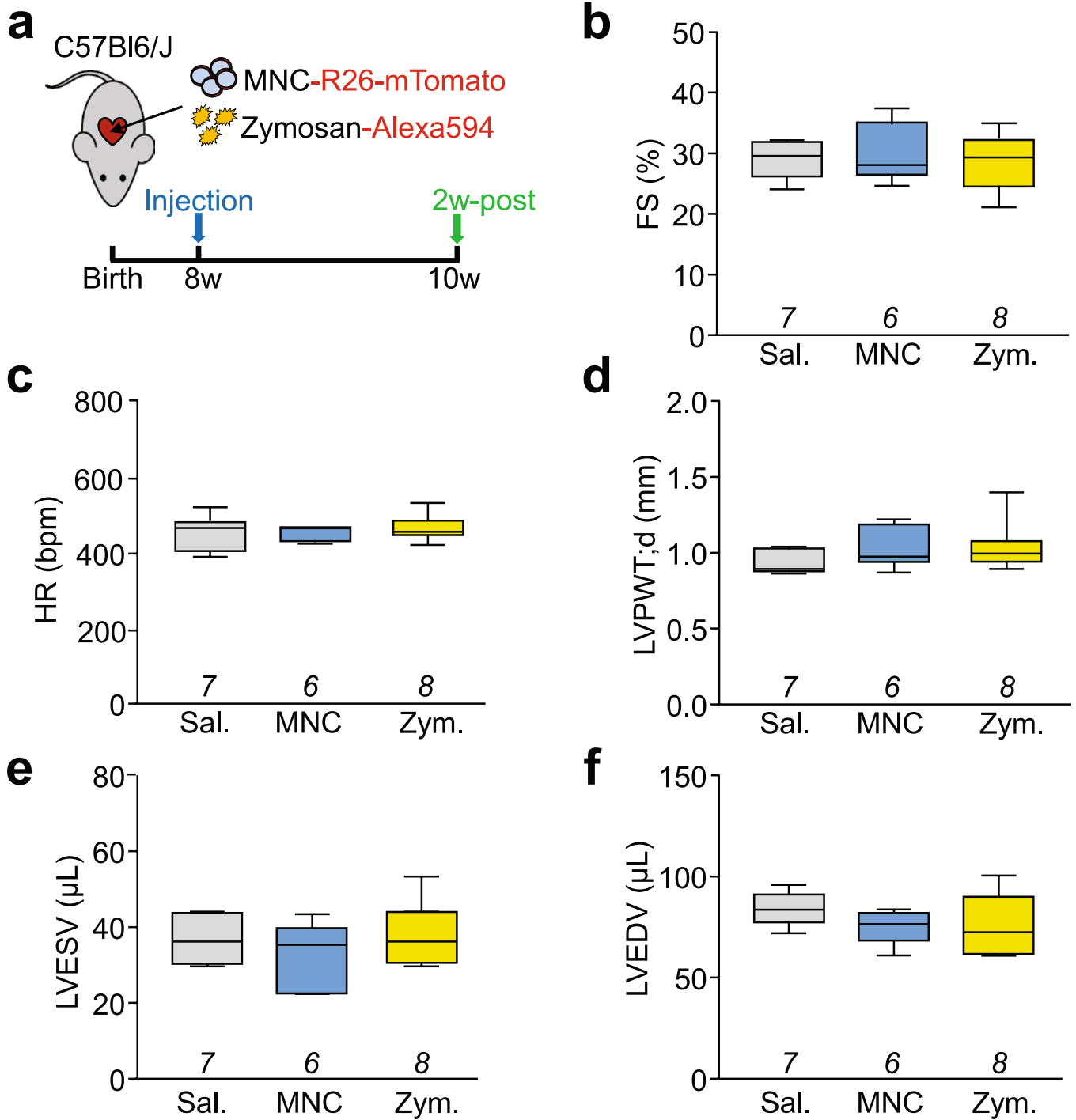
Peer review information Nature thanks Merry Lindsey, Christine Mummy and the other, anonymous, reviewer(s) for their contribution to the peer review of this work.

Reprints and permissions information is available at <http://www.nature.com/reprints>.



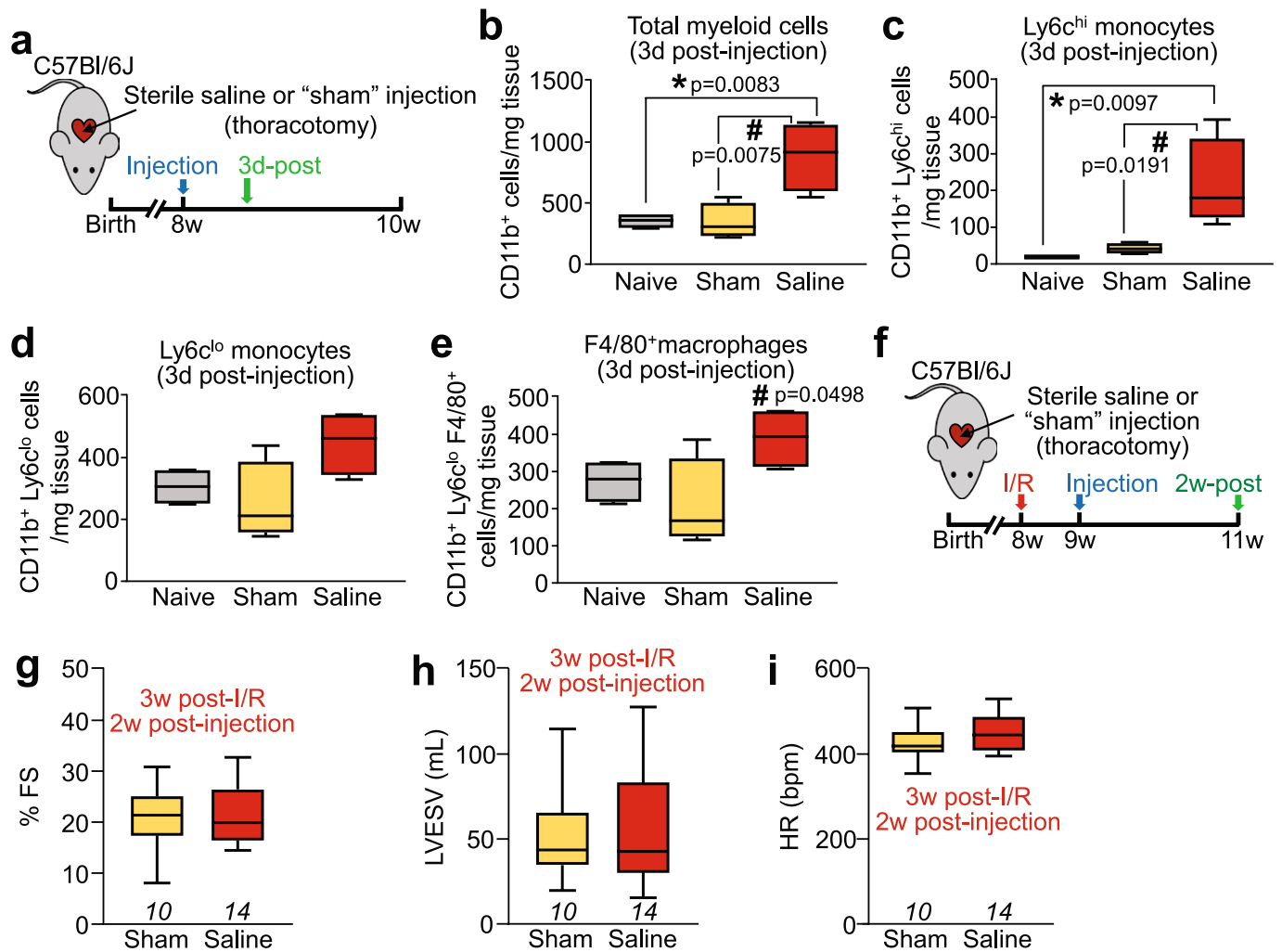
Extended Data Fig. 1 | Characterization of cells used in the injection studies and initial neutrophil response to injections. a, Flow cytometry analysis of MNCs isolated from *Rosa26-mTomato* mice for intracardiac injection. Singlet cells were selected by forward and side scatter properties followed by mTomato-positivity. mTomato⁺ cells were then assessed for surface expression of CD3e, CD11b, Ly6c, CD45R, Ly6G or Ter119 via antibodies. **b,** Flow cytometry plots for CPCs immunolabelled with antibodies against mesenchymal (Sca1), endothelial (CD31) or haematopoietic (CD45) lineage markers as indicated in the plots. An unstained negative control (unst.) plot is also shown. Gating was determined versus unstained negative controls. Similar results in **a, b** were

obtained from at least three independent cell preparations. **c,** Quantification via flow cytometry of total neutrophil levels in dissociated hearts from MNC-, zymosan- or saline-injected male and female C57Bl/6J mice, three days after injection. As a comparison, data from *n* = 5 C57Bl/6J mice isolated one day after I-R injury are also shown when neutrophil levels are high. Data are from *n* = 4 (MNC and zymosan) or *n* = 2 (saline) mice. Numerical data are summarized as box-and-whisker plots, indicating the median value (black bar inside box), 25th and 75th percentiles (bottom and top of box, respectively), and minimum and maximum values (bottom and top whisker, respectively).



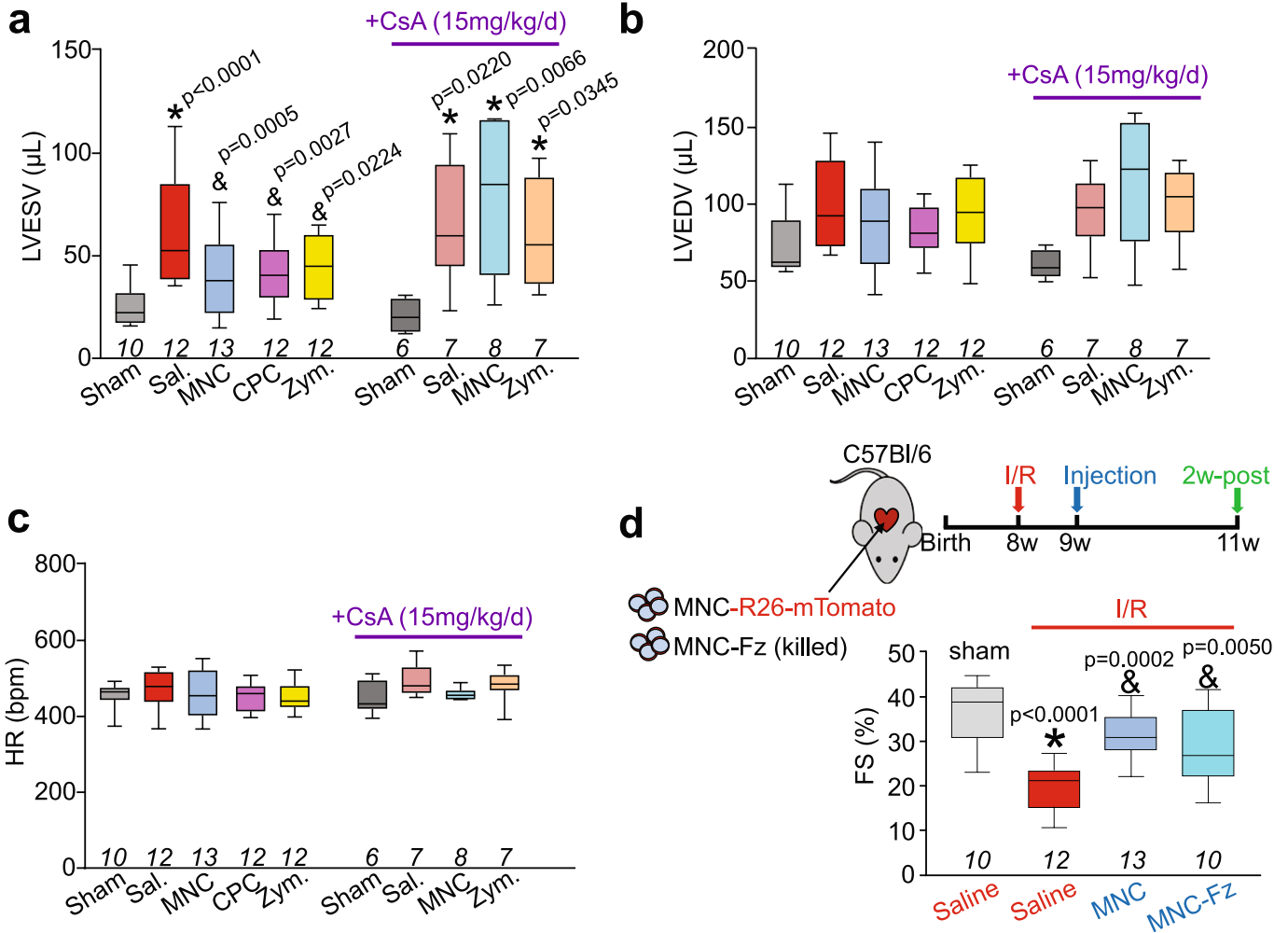
Extended Data Fig. 2 | Basal cardiac structure and function after cell or zymosan injection in uninjured mice. **a**, Schematic of all experiments performed in this figure, in which C57Bl/6J eight-week-old male and female mice received intracardiac injection of mTomato-labelled MNCs, Alexa 594-labelled zymosan or sterile saline and were assessed by echocardiography after two weeks. **b-f**, Echocardiography-measured fractional shortening (FS) percentage (**b**), heart rate (HR) as beats per minute (bpm) under isoflurane anaesthesia (**c**), left ventricular posterior wall thickness

in diastole (LVPWT;d) in millimetres (**d**), left ventricular end-systolic volume (LVESV) in microlitres (**e**) and left ventricular end-diastolic volume (LVEDV) in microlitres (**f**). All values in **b-f** were unchanged with injection of MNCs or zymosan versus saline. All numerical data are summarized as box-and-whisker plots, indicating the median value (black bar inside box), 25th and 75th percentiles (bottom and top of box, respectively), and minimum and maximum values (bottom and top whisker, respectively). The number of mice for each group in **b-f** is indicated below each respective box-and-whisker plot.



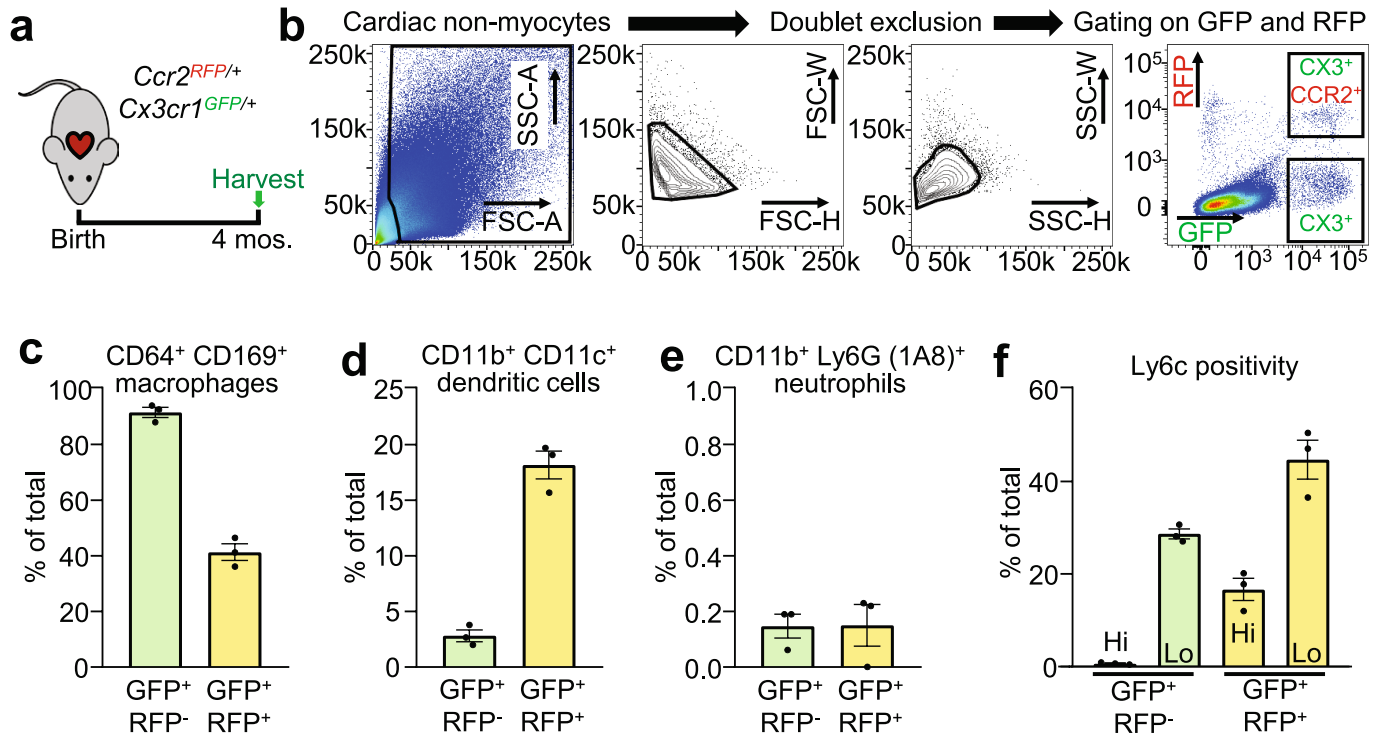
Extended Data Fig. 3 | Characterization of inflammatory and functional effects of the intracardiac injection protocol. **a**, Schematic of experiments performed in **b–e**. Eight-week-old C57Bl/6J (uninjured) male and female mice received intracardiac injection of sterile saline, or a sham procedure in which the heart was exposed by thoracotomy but no intracardiac injections were done. Naive mice without surgery served as an additional control. **b–e**, Quantification via flow cytometry of immune cells from enzymatically dissociated hearts from the above groups of mice. Total CD11b⁺ myeloid cells (**b**), CD11b⁺Ly6C^{high} (**c**) or CD11b⁺Ly6C^{low} (**d**) monocytes, and CD11b⁺F4/80⁺ macrophages (**e**) from $n = 4$ mice per group are shown, normalized to the starting weight of dissociated tissue. * $P < 0.05$ versus naive and # $P < 0.05$ versus sham by one-way ANOVA with Tukey's post hoc test (exact P values are shown in

the panel). **f**, Schematic of experiments performed in **g–i** in which eight-week-old male and female C57Bl/6J mice received I–R injury followed by either intracardiac injection of saline or thoracotomy (sham) after one week, and then were assessed by echocardiography two weeks later. **g–i**, Fractional shortening (**g**), left ventricular end-systolic volume (**h**) and heart rate under isoflurane anaesthesia (**i**), as measured by echocardiography in the groups indicated. The number of mice for each group is indicated in each graph in **g–i**. All numerical data in this figure are summarized as box-and-whisker plots, indicating the median value (black bar inside box), 25th and 75th percentiles (bottom and top of box, respectively), and minimum and maximum values (bottom and top whisker, respectively).



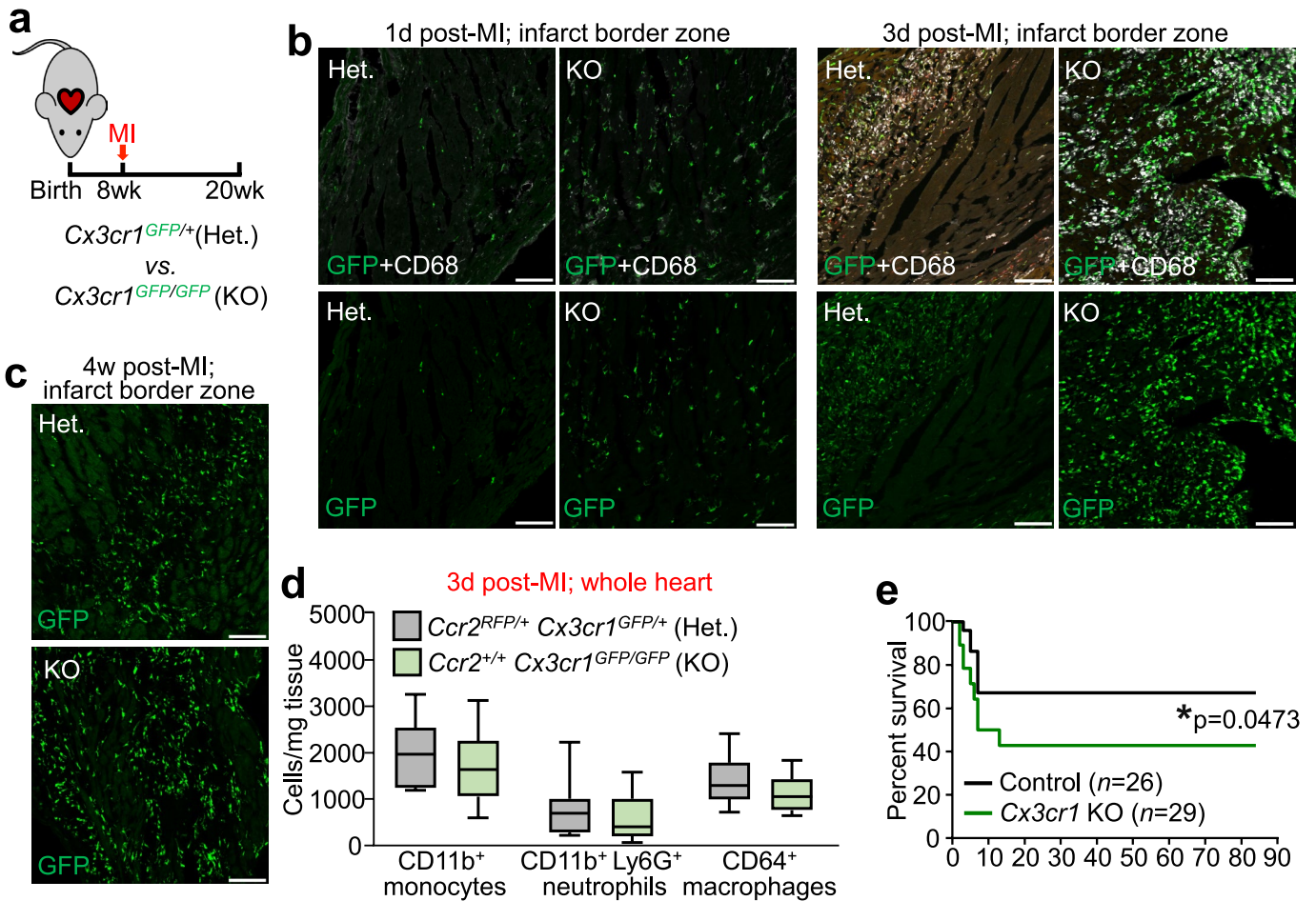
Extended Data Fig. 4 | Additional echocardiographic parameters and effect of treatment with MNCs killed by freezing and thawing, after I-R injury.
a–c, Echocardiography to measure left ventricular end-systolic volume in microlitres (**a**), left ventricular end-diastolic volume in microlitres (**b**) or heart rate under isoflurane anaesthesia (**c**) in mice that received an intracardiac injection of MNCs, CPCs, zymosan or sterile saline, three weeks after I-R. These data were collected in the same group of mice shown in Fig. 3b, d. Data in **a** are significantly different, as assessed by one-way ANOVA with Dunnett's post hoc test (exact P values are shown in the panels). **d**, Schematic of experiment in which mice received an intracardiac injection of mTomato⁺ MNCs or MNCs killed by freezing and thawing one week after I-R, and then two weeks later the

cardiac ventricular fractional shortening percentage was measured by echocardiography. Exact P values are shown in the panel versus I-R and saline, which involved one-way ANOVA with Dunnett's post hoc test to examine significance. The sham, I-R and saline, and I-R and MNC groups shown here in **d** are the same data as also shown in Fig. 3, as these studies were performed in parallel. All numerical data are summarized as box-and-whisker plots, indicating the median value (black bar inside box), 25th and 75th percentiles (bottom and top of box, respectively), and minimum and maximum values (bottom and top whisker, respectively). The number of mice for each group is indicated below the respective plot.



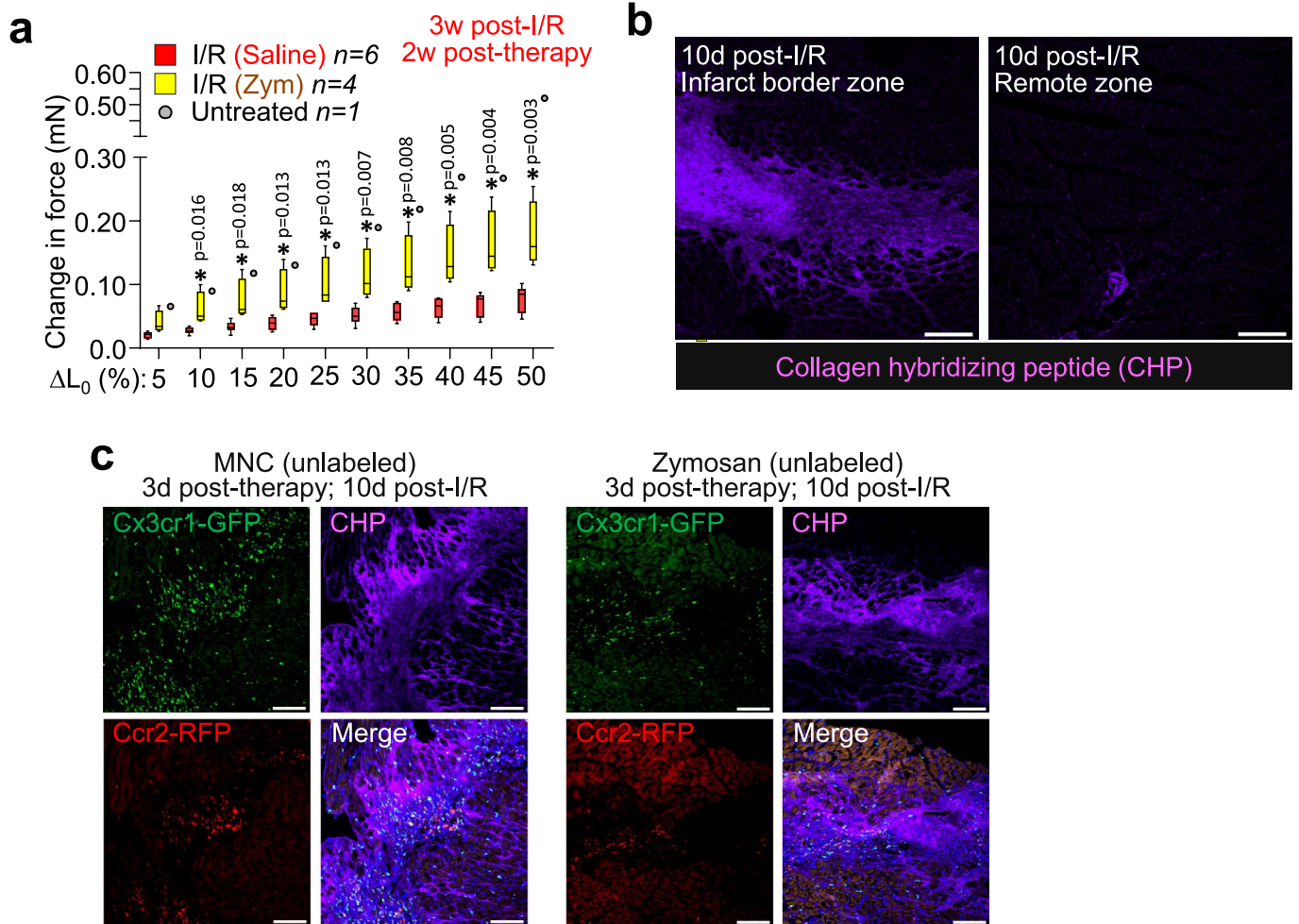
Extended Data Fig. 5 | Characterization of cell types labelled from *Ccr2-RFP* × *Cx3cr1-GFP* knock-in mice. **a**, Schematic of experiments in which hearts from male and female double-heterozygous *Ccr2-RFP* × *Cx3cr1-GFP* knock-in mice ($n = 3$) were isolated and analysed by flow cytometry at 4 months of age. **b**, Representative flow cytometry plots with the gating strategy shown, in which singlet cells were first selected by forward and side scatter properties followed by gating on endogenous GFP and RFP fluorescence for

CX3CR1⁺*CCR2*⁻ (GFP⁺RFP⁻) or *CX3CR1*⁺*CCR2*⁺ (GFP⁺RFP⁺) cells. **c-f**, Cells within the GFP⁺RFP⁻ or GFP⁺RFP⁺ gates as shown in **b** were then assessed for surface marker expression via antibodies. CD64⁺CD169⁺ macrophages (**c**), CD11b⁺CD11c⁺ dendritic cells (**d**) or CD11b⁺Ly6G⁺ neutrophils (**e**) are shown as percentage of all GFP⁺RFP⁻ or GFP⁺RFP⁺ cells. **f**, Ly6c positivity in the total GFP⁺RFP⁻ or GFP⁺RFP⁺ populations is also shown. All data are represented as the mean ± s.e.m. from $n = 3$ mice.



Extended Data Fig. 6 | Response of *Cx3cr1* global gene-deleted mice to myocardial infarction injury. **a**, Schematic of experiments in which eight-week-old male and female *Cx3cr1-GFP* heterozygous (het.) or *Cx3cr1-GFP/GFP* homozygous (knockout, KO) mice received myocardial infarction (MI) via permanent occlusion of the left coronary artery and were then followed out for 12 weeks. **b, c**, Representative confocal immunohistochemistry images from hearts of mice described in **a** at one day, three days or four weeks after myocardial infarction, showing endogenous GFP fluorescence from the *Cx3cr1* knock-in allele. Immunohistochemistry for activated CD68 macrophages (white) is also shown in **b**. Micrographs are representative of $n=3$ mice per time point. Scale bars, 100 μm . **d**, Quantification via flow cytometry of total

monocyte, neutrophil and macrophage levels in dissociated whole hearts from *Cx3cr1* heterozygous or knockout mice at three days after myocardial infarction. Data are from $n=11$ (heterozygous) or $n=12$ (knockout) mice. Numerical data are summarized as box-and-whisker plots, indicating the median value (black bar inside box), 25th and 75th percentiles (bottom and top of box, respectively), and minimum and maximum values (bottom and top whisker, respectively). **e**, Survival curve for *Cx3cr1-GFP/GFP* mice versus controls over 12 weeks (x axis shows days) after myocardial infarction injury. Control mice in this experiment included both *Cx3cr1-GFP* heterozygous and C57Bl/6J animals. The number (n) of mice for each group is indicated in the figure. * $P=0.0473$ by two-sided Gehan-Breslow-Wilcoxon test.



Extended Data Fig. 7 | Mechanical and structural improvements in cell-therapy- or zymosan-treated hearts after I-R. **a**, Change in passive force generation over increasing stretch lengthening (per cent of L_0) in isolated infarct strips from zymosan- or saline-injected hearts, analysed three weeks after surgical injury (injection of zymosan or saline occurred two weeks before collecting from mice). Exact *P* values are shown in the panel, which were determined by unpaired two-tailed *t*-test. The I-R and saline, and untreated control, data shown here are the same as in Fig. 4, as these studies were performed in parallel. Numerical data are summarized as box-and-whisker plots, indicating the median value (black bar inside box), 25th and 75th percentiles (bottom and top of box, respectively), and minimum and maximum values (bottom and top whisker, respectively), from the number (*n*) of mice indicated in the panels. **b**, Representative confocal micrographs from heart

histological sections from *Ccr2-RFP* × *Cx3cr1-GFP* mice at ten days after I-R, showing the infarct border zone versus remote myocardium, and labelled with a biotin-conjugated CHP that detects immature or denatured collagen. CHP labelling was detected with a streptavidin-conjugated Alexa 647 secondary antibody (purple). **c**, Representative confocal micrographs of heart histological sections from the post-I-R border zone of *Ccr2-RFP* × *Cx3cr1-GFP* mice that received intracardiac injection of MNCs or zymosan at seven days after I-R, analysed after an additional three days. Endogenous RFP (red) or GFP (green) fluorescence shows CCR2⁺ or CX3CR1⁺ macrophages, respectively. Sections were treated with CHP (purple) as in **b** to visualize immature collagen and areas of active remodelling versus areas in which subtypes of macrophage differentially localize. Images in **b**, **c** are representative of *n* = 2 mice per group. Scale bars, 100 μm.

Life Sciences Reporting Summary

Nature Research wishes to improve the reproducibility of the work that we publish. This form is intended for publication with all accepted life science papers and provides structure for consistency and transparency in reporting. Every life science submission will use this form; some list items might not apply to an individual manuscript, but all fields must be completed for clarity.

For further information on the points included in this form, see [Reporting Life Sciences Research](#). For further information on Nature Research policies, including our [data availability policy](#), see [Authors & Referees](#) and the [Editorial Policy Checklist](#).

Please do not complete any field with "not applicable" or n/a. Refer to the help text for what text to use if an item is not relevant to your study.

For final submission: please carefully check your responses for accuracy; you will not be able to make changes later.

ü Experimental design

1. Sample size

Describe how sample size was determined.

Sample sizes were chosen based on extensive prior experience of the lab in characterizing cardiac injury models in the mouse, including observed post-operative surgical mortality rates for myocardial infarction and ischemia/reperfusion injury.

2. Data exclusions

Describe any data exclusions.

Data exclusions were only made in the case of animals that either did not survive a given surgical procedure (intra-cardiac injection and/or myocardial infarction with reperfusion; I/R) or were insufficiently reperfused at the time of surgery (failure of surgical slipknot release). In these cases, any previously recorded data from these animals (for example at timepoints prior to death), were not excluded.

3. Replication

Describe the measures taken to verify the reproducibility of the experimental findings.

The results of all in vivo experiments were reproducible as shown across multiple animals (exact n values indicated in the text and figures) over multiple surgical cohorts. Cohorts of mice for intra-cardiac injection of cells/zymosan included age, strain, and sex-matched controls (saline injection) for comparison.

4. Randomization

Describe how samples/organisms/participants were allocated into experimental groups.

All experimental groups were allocated to provide a roughly equal mix of males and females. Randomization of mice within a group to receive a given surgical procedure (I/R or MI vs sham) or treatment (saline vs cells vs zymosan) was not needed because the mice within a given genotype or treatment group were genetically identical and were littermates.

5. Blinding

Describe whether the investigators were blinded to group allocation during data collection and/or analysis.

Full blinding during intra-cardiac injection and/or I/R injury and collection of echocardiographic data was not performed due to logistical issues of animal handling and post-operative care. Analysis of echocardiographic data, all histological analyses, gene expression analysis, and analysis of tissue passive force properties were performed by investigators blinded to experimental treatment or procedure.

Note: all in vivo studies must report how sample size was determined and whether blinding and randomization were used.

6. Statistical parameters

For all figures and tables that use statistical methods, confirm that the following items are present in relevant figure legends (or in the Methods section if additional space is needed).

n/a Confirmed

- The exact sample size (n) for each experimental group/condition, given as a discrete number and unit of measurement (animals, litters, cultures, etc.)
- A description of how samples were collected, noting whether measurements were taken from distinct samples or whether the same sample was measured repeatedly
- A statement indicating how many times each experiment was replicated
- The statistical test(s) used and whether they are one- or two-sided
Only common tests should be described solely by name; describe more complex techniques in the Methods section.
- A description of any assumptions or corrections, such as an adjustment for multiple comparisons
- Test values indicating whether an effect is present
Provide confidence intervals or give results of significance tests (e.g. P values) as exact values whenever appropriate and with effect sizes noted.
- A clear description of statistics including central tendency (e.g. median, mean) and variation (e.g. standard deviation, interquartile range)
- Clearly defined error bars in all relevant figure captions (with explicit mention of central tendency and variation)

See the web collection on [statistics for biologists](#) for further resources and guidance.

ü Software

Policy information about [availability of computer code](#)

7. Software

Describe the software used to analyze the data in this study.

Quantitation of immunohistochemistry images was performed using NIS Elements v4.50 (Nikon Instruments). Quantitation of histological images of fibrosis was performed using Adobe Photoshop CS5. Analysis of echocardiographic data was performed using VevoLAB v1.7.1. (VisualSonics). Analysis of analytical flow cytometry data was performed using FlowJo V.10 (Tree Star, Inc). Acquisition of passive tissue force measurements was performed using DMC v600A (Aurora Scientific). For statistical analysis, two-tailed t-tests (Figures 4d, 4e) were performed using Microsoft Excel, Office365 version. All other tests, including one-way analysis of variance (ANOVA), survival curve analysis, and normality tests, were performed using GraphPad Prism version 8.0.1.

For manuscripts utilizing custom algorithms or software that are central to the paper but not yet described in the published literature, software must be made available to editors and reviewers upon request. We strongly encourage code deposition in a community repository (e.g. GitHub). *Nature Methods* [guidance for providing algorithms and software for publication](#) provides further information on this topic.

ü Materials and reagents

Policy information about [availability of materials](#)

8. Materials availability

Indicate whether there are restrictions on availability of unique materials or if these materials are only available for distribution by a third party.

Kit-MerCreMer x R-GFP mice used for lineage tracing will be made available under a materials transfer agreement (MTA) between the requesting institution and Cincinnati Children's Hospital. All other materials and reagents were obtained from commercial sources (see Online Methods for full description).

9. Antibodies

Describe the antibodies used and how they were validated for use in the system under study (i.e. assay and species).

All antibodies used in this study are commercially available. Antibody validation was performed by the individual manufacturer; validation information can be found on the manufacturers' web pages via the links provided below. Please also see Supplementary Table 1 and Online Methods for further description of antibodies, including dilutions used. Staining of samples in this study was also compared to unstained or secondary antibody-only controls processed in the same way.

Individual validation statements:

Abcam: <https://www.abcam.com/primary-antibodies/improving-reproducibility-with-better-antibodies>

Thermo Fisher: <https://www.thermofisher.com/us/en/home/life-science/antibodies/invitrogen-antibody-validation.html>

Novus: <https://www.novusbio.com/5-pillars-validation>

BioLegend: <https://www.biolegend.com/reproducibility>

eBioscience: <https://www.thermofisher.com/us/en/home/life-science/antibodies/invitrogen-antibody-validation.html>

Assay: Immunohistochemistry

CD68 - Figures 1b, 1c, 3i, Extended Data Figure 6b.

Supplier: Abcam, #ab53444

Monoclonal, clone FA-11

Lot: GR3241798-1

Manufacturer's validation information: <https://www.abcam.com/cd68-antibody-fa-11-ab53444.pdf>

Dilution used here: 1:100

Detected with:

Goat anti-rat IgG Alexa Fluor 488 (Figures 1b, 1c)

Supplier: Life Technologies, #A-11006

Lot: 1887148

Manufacturer's validation information: https://assets.thermofisher.com/TFS-Assets/LSG/certificate/Certificates-of-Analysis/1887148_A11006.pdf

Dilution used here: 1:200

or

Goat anti-rat IgG Alexa Fluor 647 (Figure 3i, Extended Data Figure 6b)

Supplier: Life Technologies, #A-21247

Lot: 2043368

Manufacturer's validation information: <https://assets.thermofisher.com/TFS-Assets/BID/certificate/Certificates-of-Analysis/A21247%20Lot%202043368%20CofA.pdf>

Dilution used here: 1:200

Ki-67 - Figures 2b, 2c.

Supplier: Thermo Fisher, #14-5698-82

Monoclonal, clone SolA15

Lot: 4328926

Manufacturer's validation information: https://www.thermofisher.com/order/genome-database/dataSheetPdf?producttype=antibody&productsubtype=antibody_primary&productId=14-5698-82&version=65

Dilution used here: 1:100

Detected with:

Goat anti-rat IgG Alexa Fluor 647

Supplier: Life Technologies, #A-21247

Lot: 2043368

Manufacturer's validation information: <https://assets.thermofisher.com/TFS-Assets/BID/certificate/Certificates-of-Analysis/A21247%20Lot%202043368%20CofA.pdf>

Dilution used here: 1:200

PCM1- Figures 2b, 2c.

Supplier: Novus Biologicals, #NBP1-87196

Polyclonal

Lot: F117419

Manufacturer's validation information: <https://www.novusbio.com/PDFs/NBP1-87196.pdf>

Dilution used here: 1:100

Detected with:

Goat anti-rabbit IgG Alexa Fluor 488

Life Sciences Reporting Summary (Antibodies section did not have enough room)

9. Antibodies

Describe the antibodies used and how they were validated for use in the system under study (i.e. assay and species).

All antibodies used in this study are commercially available. Antibody validation was performed by the individual manufacturer; validation information can be found on the manufacturers' web pages via the links provided below. Please also see Supplementary Table 1 and Online Methods for further description of antibodies, including dilutions used. Staining of samples in this study was also compared to unstained or secondary antibody-only controls processed in the same way.

Individual validation statements:

Abcam: <https://www.abcam.com/primary-antibodies/improving-reproducibility-with-better-antibodies>

Thermo Fisher: <https://www.thermofisher.com/us/en/home/life-science/antibodies/invitrogen-antibody-validation.html>

Novus: <https://www.novusbio.com/5-pillars-validation>

BioLegend: <https://www.biolegend.com/reproducibility>

eBioscience: <https://www.thermofisher.com/us/en/home/life-science/antibodies/invitrogen-antibody-validation.html>

Assay: Immunohistochemistry

CD68 - Figures 1b, 1c, 3i, Extended Data Figure 6b.

Supplier: Abcam, #ab53444

Monoclonal, clone FA-11

Lot: GR3241798-1

Manufacturer's validation information: <https://www.abcam.com/cd68-antibody-fa-11-ab53444.pdf>

Dilution used here: 1:100

Detected with:

Goat anti-rat IgG Alexa Fluor 488 (Figures 1b, 1c)

Supplier: Life Technologies, #A-11006

Lot: 1887148

Manufacturer's validation information: https://assets.thermofisher.com/TFS-Assets/LSG/certificate/Certificates-of-Analysis/1887148_A11006.pdf

Dilution used here: 1:200

or

Goat anti-rat IgG Alexa Fluor 647 (Figure 3i, Extended Data Figure 6b)

Supplier: Life Technologies, #A-21247

Lot: 2043368

Manufacturer's validation information: <https://assets.thermofisher.com/TFS-Assets/BID/certificate/Certificates-of-Analysis/A21247%20Lot%202043368%20CofA.pdf>

Dilution used here: 1:200

Ki-67 - Figures 2b, 2c.

Supplier: Thermo Fisher, #14-5698-82

Monoclonal, clone SolA15

Lot: 4328926

Manufacturer's validation information: https://www.thermofisher.com/order/genome-database/dataSheetPdf?producttype=antibody&productsubtype=antibody_primary&productId=14-5698-82&version=65

Dilution used here: 1:100

Detected with:

Goat anti-rat IgG Alexa Fluor 647

Supplier: Life Technologies, #A-21247

Lot: 2043368

Manufacturer's validation information: <https://assets.thermofisher.com/TFS-Assets/BID/certificate/Certificates-of-Analysis/A21247%20Lot%202043368%20CofA.pdf>

Dilution used here: 1:200

PCM1- Figures 2b, 2c.

Supplier: Novus Biologicals, #NBP1-87196

Polyclonal

Lot: F117419

Manufacturer's validation information: <https://www.novusbio.com/PDFs/NBP1-87196.pdf>

Dilution used here: 1:100

Detected with:

Goat anti-rabbit IgG Alexa Fluor 488

Supplier: Life Technologies, #A-11008

Lot: 1853312

Manufacturer's validation information: https://assets.thermofisher.com/TFS-Assets/LSG/certificate/Certificates%20of%20Analysis/1853312_A11008.pdf

Dilution used here: 1:200

CD31 – Figures 2e, 2f.

Supplier: BD Biosciences, #553370

Monoclonal, clone MEC 13.3

Lot: 6196687

Manufacturer's validation information: <http://www.bdbiosciences.com/ds/pm/tds/553370.pdf>

Dilution used here: 1:100

Detected with:

Goat anti-rat IgG Alexa Fluor 647

Supplier: Life Technologies, #A-21247

Lot: 2043368

Manufacturer's validation information: <https://assets.thermofisher.com/TFS-Assets/BID/certificate/Certificates-of-Analysis/A21247%20Lot%202043368%20CofA.pdf>

Dilution used here: 1:200

Collagen Hybridizing Peptide, Biotin Conjugate (B-CHP) - Extended Data Figures 7b, 7c

Supplier: 3Helix #BIO300

Biotin-conjugated peptide

Manufacturer's validation information: https://www.3helix.com/wp-content/uploads/2019/04/3Helix_CHP_user_guide_20190326.pdf

Dilution used here: 15uM per tissue section

Detected with:

Alexa Fluor 647 Streptavidin

Supplier: Life Technologies, #S-21374

Lot: 1990312

Manufacturer's validation information: <https://www.thermofisher.com/document-connect/document-connect.html?url=https%3A%2F%2Fassets.thermofisher.com%2FTFS-Assets%2FBID%2Fcertificate%2FCertificates-of-Analysis%2FS21374%2520Lot%25201990312%2520CofA.pdf&title=MTk5MDMxMg==>

Dilution used here: 1:200

Assay: Flow Cytometry

CD3e, CD11b, CD45R, Ly-6G, or Ter119 (eBioscience #88-7774-75, as a biotinylated panel). Extended Data Figure 1a.

CD3e: Lot # E02344-1633

CD11b: Lot # 4283483

CD45R: Lot # 4291976

Ly6G: Lot # E03072-1632

Ter199: Lot # 4283598

Supplier: eBioscience, #88-7774-75

Manufacturer's validation information: <https://assets.thermofisher.com/TFS-Assets/LSG/manuals/88-7774.pdf>

Dilution used here: 1:50 for CD3e, 1:100 for each of the other antibodies

Detected with:

Streptavidin-conjugated Brilliant Violet 421

Supplier: BD Biosciences, #563259

Lot: 6077614

Manufacturer's validation information: <http://www.bdbiosciences.com/ds/pm/tds/563259.pdf>

Dilution used here: 1:200

Brilliant Violet 421™ anti-mouse CD11b - Extended Data Figure 3b-e.

Supplier: BioLegend, #101251

Monoclonal

Lot: B260574

Manufacturer's validation information: <https://www.biolegend.com/en-us/products/brilliant-violet-421-anti-mouse-human-cd11b-antibody-7163>

Dilution used here: 1:100

Visualized directly with conjugated fluorophore.

Brilliant Violet 510™ anti-mouse Ly6c - Extended Data Figure 3c-d

Supplier: BioLegend #128033

Monoclonal

Lot: B251849

Manufacturer's validation information: <https://www.biolegend.com/en-us/products/brilliant-violet-510-anti-mouse-ly-6c-antibody-8726>

Dilution used here: 1:100

Visualized directly with conjugated fluorophore

Brilliant Violet 421™ anti-mouse CD64 (FcγRI) - Figure 1f, Extended Data Figure 5c, Extended Data Figure 6d.

Manufacturer: BioLegend, #139309

Monoclonal

Lot: B254355

Manufacturer's validation information: <https://www.biolegend.com/en-us/products/brilliant-violet-421-anti-mouse-cd64-fcγmari-antibody-8992>

Dilution used here: 1:100

Visualized directly with conjugated fluorophore

APC anti-mouse F4/80 [BM8] - Figure 1f, Extended Data Figure 3e.

Manufacturer: BioLegend, #123116

Monoclonal

Lot: B268075

Manufacturer's validation information: <https://www.biolegend.com/en-us/products/apc-anti-mouse-f4-80-antibody-4071>

Dilution used here: 1:100

Visualized directly with conjugated fluorophore

eFluor660 CD169 (Siglec-1) - Extended Data Figure 5c.

Manufacturer: Thermo Fisher Scientific, #50-5755-82

Monoclonal

Clone: SER-4

Lot: 1917798

Manufacturer's validation information: https://www.thermofisher.com/order/genome-database/dataSheetPdf?producttype=antibody&productsubtype=antibody_primary&productId=50-5755-82&version=65

Dilution used here: 1:100

Visualized directly with conjugated fluorophore

APC anti-mouse CD11b - Extended Data Figure 5d-e, Extended Data Figure 6d.

Manufacturer: eBioscience, #17-0112-82

Monoclonal

Clone: M1/70

Lot: 4339583

Manufacturer's validation information: https://www.thermofisher.com/order/genome-database/dataSheetPdf?producttype=antibody&productsubtype=antibody_primary&productId=17-0112-82&version=65

Dilution used here: 1:100

Visualized directly with conjugated fluorophore

BUV395 Hamster Anti-Mouse CD11c - Extended Data Figure 5d.

Manufacturer: BD Biosciences, #564080

Monoclonal

Clone: HL3

Lot: 8206832

Manufacturer's validation information: <http://wwwbdbiosciences.com/ds/pm/tds/564080.pdf>

Dilution used here: 1:100

Visualized directly with conjugated fluorophore

Brilliant Violet 421™ anti-mouse LY-6G - Extended Data Figure 5e, Extended Data Figure 6d.

Manufacturer: BD Biosciences, #562737

Monoclonal

Clone: 1A8

Lot: 7270577

Manufacturer's validation information: <http://wwwbdbiosciences.com/ds/pm/tds/562737.pdf>

Dilution used here: 1:100

Visualized directly with conjugated fluorophore

Brilliant Violet 421™ anti-mouse Ly6c - Extended Data Figure 5f.

Manufacturer: BioLegend, #128031

Monoclonal

Clone: HK 1.4

Lot: B266457

Manufacturer's validation information: <https://www.biolegend.com/en-ie/products/brilliant-violet-421-anti-mouse-ly-6c-antibody-8586>

Dilution used here: 1:100

Visualized directly with conjugated fluorophore

Pacific Blue anti-mouse Ly-6A/E (Sca-1) - Extended Data Figure 1b.

Manufacturer: BioLegend, #108120

Monoclonal

Clone: D7

Lot: B181741

Manufacturer's validation information: <https://www.biolegend.com/en-us/global-elements/pdf-popup/pacific-blue-anti-mouse-ly-6a-e-sca-1-antibody-3140>

Dilution used here: 1:100

Visualized directly with conjugated fluorophore

CD45-APC - Extended Data Figure 1b.

Manufacturer: BD Biosciences, #559864

Monoclonal

Clone: 30-F11

Lot: 6203964

Manufacturer's validation information: <http://wwwbdbiosciences.com/ds/pm/tds/559864.pdf>

Dilution used here: 1:100

Visualized directly with conjugated fluorophore

Brilliant Violet 421™ anti-mouse CD31 [390] - Extended Data Figure 1b.

Manufacturer: BioLegend, #102423

Monoclonal

Clone: 390

Lot: B231773

Manufacturer's validation information: <https://www.biolegend.com/en-us/products/brilliant-violet-421-anti-mouse-cd31-antibody-8599>

Dilution used here: 1:100

Visualized directly with conjugated fluorophore